arrest genes, concomitant with suppression of IκB kinases, anti-apoptotic and DNA repair genes. The results appear to represent the expression profile corresponding to 'oncogenic shock'.[39,40]

In vivo experiments showed that PEL xenografted mice without treatment tended to be heavier, both in appearance and weight. Although we could not find statistical significances between the two groups, the mean value of the body weight was higher in the control group, which was explained by the fact that untreated mice developed tumors and effusion in body cavities. Besides, the treated group apparently did not have either effusions or tumors. The survival rate was significantly better in the treated group, indicating that DHMEQ could rescue the PEL-xenografted mice.

In summary, the present work demonstrated that DHMEQ could abrogate NF-κB activation transiently and initiated the apoptosis cascade irreversibly without activation of HHV-8 replication. In addition, DHMEQ rescued the xenografted mice. Therefore, our data provided proof of the concept that DHMEQ can be a promising candidate for molecular target therapy of the PEL.

Acknowledgments

This work was supported in part by Grants-in-Aid for Scientific Research from the Ministry of Education, Culture, Sports, Science and Technology, and by a Research Grant from the Ministry of Health, Labour and Welfare, Japan.

References

1 Nador R, Cesarman E, Chadburn A *et al.* Primary effusion lymphoma: a distinct clinopathologic entity associated with the Kaposi's sarcoma associated herpes virus. *Blood* 1996; **88**: 645–56.
2 Klepfish A, Sarid R, Shtalrid M *et al.* Primary effusion lymphoma (PEL) in HIV-negative patients – a distinct clinical entity. *Leuk Lymphoma* 2001; **41**: 439–43.
3 Boulanger E, Gérard L, Gabarre J *et al.* Prognostic factors and outcome of human herpesvirus 8 – associated primary effusion lymphoma in patients with aids. *J Clin Oncol* 2005; **23**: 4372–80.
4 Hengge UR, Ruzicka T, Tyring SK *et al.* Update on Kaposi's sarcoma and other HHV8 associated diseases. Part 2: pathogenesis, Castleman's disease, and pleural effusion lymphoma. *Lancet Infect Dis* 2002; **2**: 344–52.
5 Jarviluoma A, Ojala PM. Cell signaling pathways engaged by KSHV. *Biochim Biophys Acta* 2006; **1766**: 140–58.
6 Sun Q, Matta H, Chaudhary PM. The human herpes virus 8-encoded viral FLICE inhibitory protein protects against growth factor withdrawal-induced apoptosis via NF-kappa B activation. *Blood* 2003; **101**: 1956–61.
7 Chaudhary PM, Jasmin A, Eby MT *et al.* Modulation of the NF-kappa B pathway by virally encoded death effector domains-containing proteins. *Oncogene* 1999; **18**: 5738–46.
8 Guasparri I, Keller SA, Cesarman E. KSHV vFLIP is essential for the survival of infected lymphoma cells. *J Exp Med* 2004; **199**: 993–1003.
9 Keller SA, Schattner EJ, Cesarman E. Inhibition of NF-kappaB induces apoptosis of KSHV-infected primary effusion lymphoma cells. *Blood* 2000; **96**: 2537–42.
10 Keller SA, Hernandez-Hopkins D, Vider J *et al.* NF-κB is essential for progression of KSHV- and EBV-infected lymphomas in vivo. *Blood* 2006; **107**: 3295–302.
11 Chen LF, Greene WC. Shaping the nuclear action of NF-kappaB. *Nat Rev Mol Cell Biol* 2004; **5**: 392–401.
12 Chen LF, Greene WC. Regulation of distinct biological activities of the NF-kappaB transcription factor complex by acetylation. *J Mol Med* 2003; **81**: 549–57.
13 Matsumoto N, Ariga A, To-e S *et al.* Synthesis of NF-kappaB activation inhibitors derived from epoxyquinomicin C. *Bioorg Med Chem Lett* 2000; **10**: 865–9.
14 Umezawa K, Chaicharoenpong C. Molecular design and biological activities of NF-kappaB inhibitors. *Mol Cells* 2002; **14**: 163–7.
15 Watanabe M, Ohsugi T, Shoda M *et al.* Dual targeting of transformed and untransformed HTLV-1-infected T cells by DHMEQ, a potent and selective inhibitor of NF-kappaB, as a strategy for chemoprevention and therapy of adult T-cell leukemia. *Blood* 2005; **106**: 2462–71.
16 Watanabe M, Dewan Md. Z, Taira M *et al.* IκBα independent induction of NF-κB and its inhibition by DHMEQ in Hodgkin-Reed-Sternberg cells. *Lab Invest* 2007; **87**: 372–82.
17 Horie R, Watanabe M, Okamura T *et al.* DHMEQ, a new NF-kappaB inhibitor, induces apoptosis and enhances fludarabine effects on chronic lymphocytic leukemia cells. *Leukemia* 2006; **20**: 800–6.
18 Watanabe M, Dewan Md Z, Okamura T *et al.* A novel NF-kappaB inhibitor DHMEQ selectively targets constitutive NF-kappaB activity and induces apoptosis of multiple myeloma cells *in vitro* and *in vivo*. *Int J Cancer* 2005; **114**: 32–8.
19 Nishimura D, Ishikawa H, Matsumoto K *et al.* DHMEQ, a novel NF-kappaB inhibitor, induces apoptosis and cell-cycle arrest in human hepatoma cells. *Int J Oncol* 2006; **29**: 713–9.
20 Matsumoto G, Muta M, Umezawa K *et al.* Enhancement of the caspase-independent apoptotic sensitivity of pancreatic cancer cells by DHMEQ, an NF-kappaB inhibitor. *Int J Oncol* 2005; **27**: 1247–55.
21 Matsumoto G, Namekawa J, Muta M *et al.* Targeting of nuclear factor kappaB pathways by dehydroxymethylepoxyquinomicin, a novel inhibitor of breast carcinomas: antitumor and antiangiogenic potential *in vivo*. *Clin Cancer Res* 2005; **11**: 1287–93.
22 Drexler HG, Uphoff CC, Gaidano G, Carbone A. Lymphoma cell lines: *in vitro* models for the study of HHV-8$^+$ primary effusion lymphomas (body cavity-based lymphomas). *Leukemia* 1998; **12**: 1507–17.
23 Katano H, Hoshino Y, Morishita Y *et al.* Establishing and characterizing a CD30-positive cell line harboring HHV-8 from a primary effusion lymphoma. *J Med Virol* 1999; **58**: 394–401.
24 Lenardo MJ, Baltimore D. NF-kappaB: A pleiotropic mediator inducible and tissue-specific gene control. *Cell* 1989; **58**: 227–9.
25 Andrews NC, Faller DV. A rapid micropreparation technique for extraction of DNA-binding proteins from limiting numbers of mammalian cells. *Nucl Acids Res* 1991; **19**: 2499.
26 Miyake A, Dewan MdZ, Ishida T *et al.* Induction of apoptosis in Epstein-Barr virus-infected B-lymphocytes by the NF-κB inhibitor DHMEQ. *Microbes Infect* 2008; **10**: 748–56.
27 Krishnan HH, Naranatt PP, Smith MS *et al.* Concurrent expression of latent and a limited number of lytic genes with immune modulation and antiapoptotic function by Kaposi's sarcoma-associated herpesvirus early during infection of primary endothelial and fibroblast cells and subsequent decline of lytic gene expression. *J Virol* 2004; **78**: 3601–20.
28 Yoo SM, Zhou FC, YeFC *et al.* Early and sustained expression of latent and host modulating genes in coordinated transcriptional program of KSHV productive primary infection of human primary endothelial cells. *Virology* 2005; **343**: 47–64.
29 O'Donovan M, Silva I, Uhlmann V *et al.* Expression profile of human herpesvirus 8 (HHV-8) in pyothorax associated lymphoma and in effusion lymphoma. *Mol Pathol* 2001; **54**: 80–5.
30 Ghosh SK, Wood C, Boise LH *et al.* Potentiation of TRAIL-induced apoptosis in primary effusion lymphoma through azidothymidine-mediated inhibition of NF-kappaB. *Blood* 2003; **101**: 2321–7.
31 Brown HJ, Song MJ, Deng H *et al.* NF-kappaB inhibits gammaherpesvirus lytic replication. *J Virol* 2003; **77**: 8532–40.
32 Ohsugi T, Horie R, Kumasaka T *et al.* *In vivo* antitumor activity of the NF-kB inhibitor dehydroxymethylepoxyquinomicin in a mouse model of adult T-cell leukemia. *Carcinogenesis* 2005; **26**: 1382–8.
33 Ohsugi T, Kumasaka T, Ishida A *et al.* *In vitro* and *in vivo* antitumor activity of the NF-κB inhibitor DHMEQ in the human T-cell leukemia virus type 1-transformed cell line, HUT-102. *Leuk Res* 2006; **30**: 90–7.
34 Liu L, Eby MT, Rathore N *et al.* The human herpes virus 8-encoded viral FLICE inhibitory protein physically associates with and persistently activates the IkappaB kinase complex. *J Biol Chem* 2002; **277**: 13745–51.
35 Field N, Low W, Daniels M *et al.* KSHV vFLIP binds to IKK-gamma to activate IKK. *J Cell Sci* 2003; **116**: 3721–8.
36 Pierce JW, Schoeenleber R, Jesmok G *et al.* Novel inhibitors of cytokine-induced IkappaB-alpha phosphorylation and endothelial cell adhesion molecule expression show anti-inflammatory effects *in vivo*. *J Biol Chem* 1997; **272**: 21096–103.
37 Berger N, Bassat HB, Klein BY, Laskov R. Cytotoxicity of NF-κB inhibitors Bay 11-7085 and caffeic acid phenethyl ester to Ramos and other human B-lymphoma cell lines. *Exp Hemaol* 2007; **35**: 1495–509.
38 Weinstein IB. Disorders in cell circuitry during multi-stage carcinogenesis. *Caricinogenesis* 2000; **21**: 857–64.
39 Sharma SV, Fischbach MA, Haber DA, Settleman J. 'Oncogene shock' explaining oncogene addiction through differential signal activation. *Clin Cancer Res* 2006; **12** (14 Suppl.): 4392s–95s.
40 Sharma SV, Settleman J. Oncogene addiction: setting the stage for molecularly targeted cancer therapy. *Genes Dev* 2007; **21**: 3214–31.
41 Nieminen AI, Partanen JI, Klefstrom J. c-Myc blazing a trail of death:

coupling of the mitochondrial and death receptor apoptosis pathways by c-Myc. *Cell Cycle* 2007; **6**: 2464–72.
42 Cory S, Adams JM. The Bcl2 family: regulators of the cellular life-or-death switch. *Nat Rev Cancer* 2002; **2**: 647–56.
43 Cowling V, Downward J. Caspase-6 is the direct activator of caspase-8 in the cytochrome c-induced apoptosis pathway: absolute requirement for removal of caspase-6 prodomain. *Cell Death Differ* 2002; **9**: 1046–56.
44 Sgarbanti M, Arguello M, Tenover BR *et al.* A requirement for NF-kappaB induction in the production of replication-component HHV-8 virions. *Oncogene* 2004; **23**: 5770–80.
45 Cahir-McFarland ED, Carter K, Rosenwald A *et al.* Role of NF-kappa B in cell survival and transcription of latent membrane protein 1-expressing or Epstein-Barr virus latency III-infected cells. *J Virol* 2004; **78**: 4108–19.

Supporting Information

Additional Supporting Information may be found in the online version of this article:

List of up-regulated genes after DHMEQ (10 μg/mL for 6 h) treatment in BC1 and BCBL1 calculated by GeneSpring software (*T*-test, *P*-value < 0.01).

Please note: Wiley-Blackwell are not responsible for the content or functionality of any supporting materials supplied by the authors. Any queries (other than missing material) should be directed to the corresponding author for the article.

doi: 10.1111/j.1349-7006.2009.01083.x

ELSEVIER

INSTITUT PASTEUR

Microbes and Infection 9 (2007) 1581–1589

www.elsevier.com/locate/micinf

Original article

Integration of HIV-1 caused STAT3-associated B cell lymphoma in an AIDS patient

Harutaka Katano [a,*], Yuko Sato [a], Satomi Hoshino [b], Natsuo Tachikawa [c], Shinichi Oka [c], Yasuyuki Morishita [d], Takaomi Ishida [e], Toshiki Watanabe [e], William N. Rom [b], Shigeo Mori [f], Tetsutaro Sata [a], Michael D. Weiden [b], Yoshihiko Hoshino [b,**]

[a] *Department of Pathology, National Institute of Infectious Diseases, 1-23-1 Toyama, Shinjuku, Tokyo 162-8640, Japan*
[b] *Division of Pulmonary and Critical Care Medicine, Department of Medicine, New York University School of Medicine, New York, NY 10016, USA*
[c] *AIDS Clinical Center, International Medical Center of Japan, Tokyo 162-8655, Japan*
[d] *Department of Pathology, Graduate School of Medicine, University of Tokyo, Tokyo 113-0033, Japan*
[e] *Department of Medical Genome Sciences, Graduate School of Frontier Sciences, University of Tokyo, Tokyo 108-8639, Japan*
[f] *Department of Pathology, Teikyo University School of Medicine, Tokyo 173-8605, Japan*

Received 26 June 2007; accepted 4 September 2007
Available online 14 September 2007

Abstract

Signal transducer and activator of transcription 3 (STAT3) is a DNA-binding transcription factor activated by multiple cytokines and interferons. High expression of STAT3 has also been implicated in cancer and lymphoma. Here, we show a case of B cell lymphoma in which a defective human immunodeficiency virus 1 (HIV-1) integrated upstream of the first STAT3 coding exon. The lymphoma cells with anaplastic large cell morphology formed multiple nodular lesions in the lung of an acquired immunodeficiency syndrome (AIDS) patient with Kaposi's sarcoma. The provirus had a 5′ long terminal repeat (LTR) deletion, but the 3′ LTR had stronger promoter activity than the STAT3 promoter in reporter assays. Immunohistochemistry showed increased expression of STAT3 in the nuclei of lymphoma cells. Transfection of STAT3 resulted in transient cell proliferation in primary B cells in vitro. Although this is a very rare case of HIV-1-integrated lymphoma, these data suggest that up-regulation of STAT3 caused by HIV-1 integration resulted in the development of B cell lymphoma in this special case.

Keywords: HIV-1; Integration; AIDS-related lymphoma; STAT3

1. Introduction

Malignant lymphoma is an important complication of patients with acquired immunodeficiency syndrome (AIDS). A large part of AIDS-related lymphomas are of B cell linage, and positive for Epstein–Barr virus (EBV) or Kaposi's sarcoma-associated herpesvirus (KSHV) [1–4]. Since human immunodeficiency virus 1 (HIV-1) is not usually detected in AIDS-related lymphoma cells, HIV-1 infection plays an indirect role in lymphomagenesis by impairing host immune surveillance. However, proviral DNA can either disrupt expression of tumor suppressor genes or enhance expression of cellular oncogenes. Alternatively, retroviral promoters can integrate into the host genome in such a manner that expression of a nearby oncogene is enhanced by a strong promoter within the proviral 3′-long terminal repeat (3′LTR). In humans, abnormal T cell proliferation following gene therapy for severe combined immunodeficiency resulted from retroviral integration into the intron of the *LMO2* proto-oncogene [5].

* Corresponding author. Tel.: +81 3 5285 1111; fax: +81 3 5285 1189.
** Corresponding author. Departments of Environmental Medicine and Medicine, New York University School of Medicine, 462 First Avenue NB 8E38, New York, NY 10016, USA. Tel.: +1 212 263 7770; fax: +1 212 263 8501.
E-mail addresses: katano@nih.go.jp (H. Katano), hoshiy01@gcrc.med.nyu.edu (Y. Hoshino).

1286-4579/$ - see front matter © 2007 Elsevier Masson SAS. All rights reserved.
doi:10.1016/j.micinf.2007.09.008

In AIDS patients, some cases of lymphomas had HIV-1 integration within the *fur* gene, just upstream from the *c-fes/fps* proto-oncogene [6]. That report, however, did not investigate the functional effect of this integration event. These observations suggest that HIV-1 may contribute directly to lymphomagenesis by inserting an active promoter into a cellular oncogene [6]. In the present study, we report a case of AIDS-related lymphoma in which HIV-1 integrated upstream of the STAT3 gene. The association of HIV-integration and lymphomagenesis was investigated.

2. Materials and methods

2.1. Samples

Lymphoma tissues in the lung of a patient with HIV-1 infection were obtained at autopsy. Formalin-fixed pathological samples of lymphoma, including nine unrelated cases of AIDS-related lymphoma and 15 cases of non-Hodgkin lymphoma in HIV-1-uninfected individuals, were studied. All samples were obtained with informed consent according to the Declaration of Helsinki. The study protocol was approved by the institutional review board of National Institute of Infectious Diseases (Approval No. 93).

2.2. Immunohistochemistry and in situ hybridization

Immunohistochemistry was performed as described before [7,8]. Primary antibodies were: anti-CD3 (Dako, Copenhagen, Denmark), CD20 (Dako), CD30 (Dako), CD45 (Dako), CD45RO (Dako), CD79a (Dako), CD138 (Serotec, Oxford, UK), and $p80^{NPM/ALK}$ (Nichirei, Tokyo, Japan), STAT3 (sc8019, Santa Cruz Biotechnology, Santa Cruz, CA), pSTAT3 (sc8059, Santa Cruz), KSHV-encoded LANA [8], and vIL-6 [7] antibodies. In situ hybridization for EBERs was performed as described before [9].

2.3. PCR and DNA sequences

PCR detection for KSHV-encoded open reading frame (ORF) 26, EBV W region, HIV-1 V3, and β-globin gene was performed as described previously [9,10]. For PCR amplification of HIV-1 3′LTR and STAT3 junction, HIV3LTR-F (5′-TCTGAGCCTGGGAGCTCTCT-3′, 9561–9580 in GenBank K03455) and Stat3intron-R (5′-AGTGCATGGCACATAACAGA-3′, 41131–41150 in GenBank AY572796) were used. For amplification of HIV-1 5′LTR and STAT3 junction, 6 reverse primers of 5′LTR (55R 5′-TCAGGGAAGTAGCCTTGTGTGTGGT-3′, 78R 5′-GCCCTGGTGTGTAGTTCTGTCAATC-3′, 348R 5′-GAAAGTCCCCAGTGGAAAGTCCCTT-3′, 495R 5′-GCAGTGGGTTCCCTAGTTAGCC-3′, 563R 5′-TTACCAGAGTCACACAACAGACGGG-3′, and 612R 5′-CACTGCTAGAGATTTTCCACACTGAC-3′), and a reverse primer positioning between 5′LTR and gag (676R 5′-CGAGTCCTGCGTCGAGAGATCTCCT-3′) were used with a forward primer of Stat3-intronF2 (5′-CATTTTTCTTTCCTTCTCTGTTGTC-3′, 40881–40905 in GenBank AY572796). These primers for HIV-1 were designed based on the sequence of HIV-1 IIIB (GenBank K03455).

2.4. Cloning of HIV-1 integration sites

The methods used were essentially as described for the Gene Walker Kit (BD Clontech, Palo Alto, CA). Lung tumor DNA was cleaved with four different blunt cutting enzymes (*Dra*I, *Eco*RV, *Pvu*II and *Ssp*I). Gene specific primers for HIV-1 LTR were 5′-ACCACACACAAGGCTACTTCCCTGA-3′ (GSP-1) and 5′-AAGGGACTTTCCACTGGGGACTTTC-3′ (GSP-2).

2.5. Real-time PCR

Copy numbers of HIV-1 integration site and STAT3 gene were measured with real time PCR as described previously [11]. Two probe and primer sets were used (Set 1: forward primer: 5′-CTAGAGATCCCTCAGACCATTTTAGTC-3′, reverse: 5′-AAAAGTATAAATGAGGATCCAGGAAGAT-3′, probe: 5′-6FAM-TGTGGAAAATCTCTAGCAGAATCTCAGG-TAMRA-3′; Set 2: forward primer: 5′-GCAGCTTGACACACGGTACCT-3′, reverse: 5′-AAACTGCCGCAGCTCCATT-3′, probe: 5′-6FAM-AGCAGCTCCATCAGCTCTACAGTGACAGC-TAMRA-3′).

2.6. Plasmids

For the promoter assay, genes of the HIV-1 3′LTR, STAT3-intron (40951–41959 of GenBank AY572796), and STAT3-promoter (1–1998 of GenBank AY572796) were amplified from DNA of the HIV-1-integrated lymphoma using the LTR-*Mlu*I-F, 5′-GAG*ACGCGT*TGGAAGGGCTAATTCACTCCC-3′ and LTR-*Xho*I-R, 5′-GTG*CTCGAG*TGCTAGAGATTTTCCACACT-3′, the Intron-*Mlu*I-F, 5′-GAG*ACGCGT*GAATCTCAGGCAGATCTTCC-3′ and Intron-*Xho*I-R, 5′-CAC*CTCGAG*CCTGCTAAAATCAGGGGTCCC-3′, and, the Stat3prom-*Mlu*F1, 5′-GAG*ACGCGT*ACCCATAGTCGCAGAGGTAGA-3′ and Stat3prom-*Xho*R1, 5′-GAG*CTCGAG*CGCTGAATTACAGCCCCTTCA-3′, respectively. Enzyme sites are indicated in italics. A fragment of the HIV-1 3′LTR was amplified also from HIV-1 pNL4-3 (GenBank AF324493). The PCR product was subcloned into *Mlu*I-*Xho*I site of pGL3-basic vector (Promega, Madison, WI). For the STAT3-expression plasmid, STAT3 cDNA was amplified from the mammalian gene collection-human (MGC-1607, American type culture collection, Manassas, VA) using forward primer (STAT3-HpaI-F10 5′-CACCGTTAACGGATCCTGGACAGGCACCC-3′) and reverse primer (STAT3-R24 5′-CATGTCAAAGGTGAGGGACTCAAA-3′). The PCR product was TA cloned using pcDNA 3.1 Directional TOPO Expression kit (Invitrogen, Carlsbad, CA). For cell proliferation experiment, the STAT3 expression vector was digested with *Hin*dIII and *Eco*RV and ligated into *Bsm*BI and *Eco*RV sites of pMACS 4-IRES.II vector, which is a bicistronic expression vector containing multiple cloning site followed by an internal ribosome entry site (IRES) element

from encephalomyocarditis virus and the truncated (non-functional) CD4 cDNA (Miltenyl Biotec, Auburn CA).

2.7. Promoter assay

Plasmids were transiently transfected into HeLa cells with a renilla reporter gene construct using Lipofectamine Plus (Invitrogen). Luciferase activity was measured with a dual luciferase assay system (Promega). In the HIV-1-Tat (+) group, an HIV-1-Tat expression vector, kindly provided by Dr. Kenzo Tokunaga, National Institute of Infectious Diseases, Tokyo, Japan, was cotransfected.

2.8. DNA methylation analysis

Methylation of the cytosine residue of the CpG site was analyzed by the bisulfite genomic sequencing method, as described previously [12]. The primer pair for selective analysis was as follows: sense primer, 5′-TATAAACCAGCATGG GATGGATGA-3′; antisense primer, 5′-CCCAGGCTCGGA TCTGGTCTAACC-3′.

2.9. Cell proliferation assay for primary lymphocytes

Primary B cells were negatively selected from whole blood of healthy volunteers using RosetteSep B cell enrichment (StemCell Technology, Vancouver, BC, Canada) [13]. Cell proliferation assay was performed using BrdU Cell proliferation ELISA kit (Roche Molecular Biochemicals, Indianapolis, IN).

3. Results

3.1. HIV-1 was concentrated in lymphoma cells in a case of AIDS-related lymphoma

A 59-year-old, homosexual, HIV-1-positive male with a CD4 cell count of 6/mm^3 showed high fever and multiple KS skin lesions. Computed tomography scanning revealed multiple nodules in the lung (Fig. 1A). Despite treatments with antibiotics and combined chemotherapy, with intensive care, he died 30 days after admission. The clinical course of the patient was also reported previously [14]. At autopsy, multiple nodules were present in the lung (Fig. 1B). Histologically, these nodules were composed of large atypical cells with anaplastic large cell morphology infiltrating into interstitial and alveolar areas in the lung tissue (Fig. 1C). Immunohistochemistry demonstrated that the tumor cells were CD3$^-$, CD20$^-$, CD30$^+$, CD45$^+$, CD45RO$^+$, CD79a$^-$, CD138$^-$, and p80$^{NPM/ALK-}$, suggesting that the lung tumor was composed of lymphoma cells (Fig. 1D and data not shown) [14]. Southern blot hybridization of DNA extracted from the lung tumor with an immunoglobulin junction hinge (JH) probe demonstrated immunoglobulin gene rearrangement, confirming a B

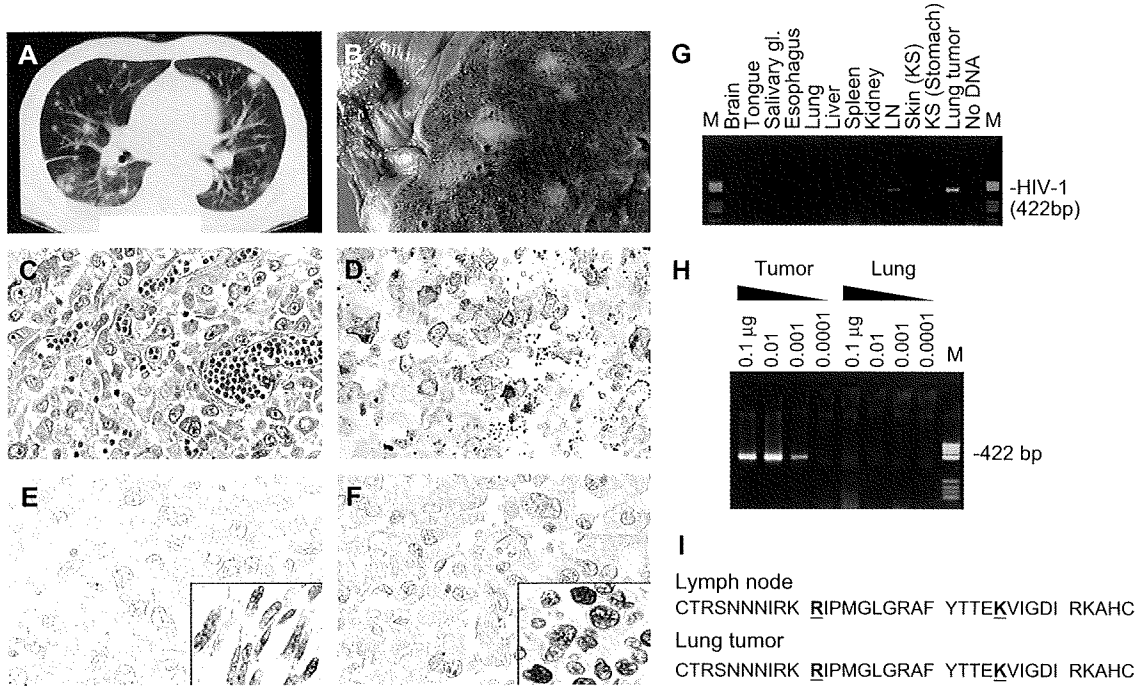

Fig. 1. Pathological findings of tumors in the lung of a patient with AIDS. CT scan (A), macroscopic view (B) and Hematoxylin and eosin staining (C) of the lung tumor. (D) Immunohistochemistry of CD45RO. (E) Immunohistochemistry for KSHV-LANA in the lung tumor cells. Inset shows gastric KS cells from the patient. (F) In situ hybridization for EBV-EBER in the lung tumor cells. Inset shows a positive control of EBV-positive lymphoma from an unrelated patient. (G) PCR detection for HIV-1 V3 region in various organs of the patient. LN, lymph node; M, DNA molecular weight marker (pBR322/*Hae*III). (H) Semi-quantitative PCR for HIV-1. DNA quantities are indicated at the top of the panel. DNA extracted from the lung tumor and surrounding lung tissues was tested. (I) Predicted amino acid sequence of HIV-1 gp120 V3 loop of HIV-1 amplified from the lymph node and lung tumor by PCR. Positions 11 and 25 are indicated by bold letters with underlines. DNA sequences are deposited in GenBank under accession numbers DQ116951 to DQ116954 (HIV-1 envelope from LN and lung tumor).

cell linage (data not shown). Since KS lesions were found in the oral cavity, stomach, sole and some lymph nodes at autopsy, we examined KSHV positivity in the lymphoma (lung tumor). KSHV-encoded ORF26 was amplified in both gastric KS lesions and lung tumor by PCR (data not shown). However, immunohistochemistry demonstrated that expression of KSHV LANA was very weak or absent in the lymphoma cells, whereas KS cells in the stomach strongly expressed LANA (Fig. 1E). Immunohistochemistry also demonstrated that the lung tumor cells were negative for KSHV-encoded vIL-6 (data not shown). The lymphoma cells were positive for EBV by PCR (data not shown), but in situ hybridization failed to detect EBERs (Fig. 1F). Thus, these data suggest that KSHV and EBV were present in the lymphoma at low copy numbers. Surprisingly, HIV-1 DNA was detected in the lymphoma cells by PCR, but not in other organs besides the lymph nodes (Fig. 1G). Semi-quantitative PCR revealed that there was a 100-fold higher copy number of HIV-1 DNA from the lymphoma than from surrounding lung tissue (Fig. 1H). PCR products of HIV-1 V3 region were TA-cloned and each 10 clones were sequenced. Although two (clones L2 and T3) and three (clones T1, T3, and T6) kinds of sequences were obtained from the lymph nodes and lymphoma, respectively, all sequences coded the same amino acid sequence in the V3 loop (net charge = + 7). Basic amino acids at positions 11 and 25 of the gp120 V3 loop and a high positive net charge strongly suggest that fusogenic X4 viruses were detected in the lymphoma cells and lymph nodes (Fig. 1I) [15].

3.2. HIV-1 integration in the STAT3 gene

A high copy number of HIV-1 in the lymphoma suggested integration of HIV-1 into the genome of lymphoma cells. Genome walking PCR produced a 400 bp fragment which contained a 300 bp fragment with >99% identity with the HIV-1 IIIB 3′LTR sequence (GenBank K03455) and A 40 bp genomic segment just before the first coding exon of STAT3 (Fig. 2A). PCR using primers in HIV-1 3′LTR and STAT3-intron yielded an independent amplicon with HIV-1 3′LTR and the predicted STAT3 genomic sequences from DNA of the lymphoma cells (Fig. 2B). These data confirmed that HIV-1 had integrated into the intervening sequence just before the first coding exon of STAT3. PCR using a primer pair binding to the STAT3 intron and upstream of HIV-1 gag demonstrates that the 5′LTR of the integrated HIV-1 was truncated (Fig. 2C). The sequence analysis revealed that the integrated HIV-1 lacked a fragment at the position of 1–587 in the 5′LTR (Fig. 2A,D, GenBank AF538307). Compared with the sequence of the 3′ integration site, HIV-1 integration resulted in duplication of the cellular 5 bp (GAATC) and addition of a dinucleotide at the integration site by HIV-1 integrase, which is commonly seen among retrovirus integrases [16,17]. Consequently, the integration event was produced by a defective virus (Fig. 2A,D). The absence of p24-staining of the tumor is consistent with this conclusion (data not shown).

3.3. Copy number of the integrated HIV-1 in the lymphoma tissue

Generally, pathological tissues obtained from lymphoma lesions contain not only lymphoma cells, but also surrounding CD4-positive T cells or alveolar macrophages. Although immunohistochemistry demonstrated no or rare CD4-positive cells in the lymphoma tissue, we tried to determine a copy number of the integrated HIV-1 in the lymphoma tissue by a real time PCR targeting genes near the integration site to deny the possibility that HIV-1 integration was originated in the contaminated CD4-positive cells (Fig. 3). A fragment of HIV-1-integration site was amplified at 12,570 copies/100 ng of DNA by the real time PCR, whereas exon 1 of STAT3 gene was amplified at 121,597 copies/100 ng. Since each cell has two copies of STAT3 gene on two alleles, these data suggest that HIV-1 integration occurred about 20% of the population that the DNA was extracted from. As shown in Fig. 1C, the lymphoma tissue contained many cells other than lymphoma cells, such as alveolar epithelial cells, macrophages, and endothelial cells. However, CD4-positive T cells were rare in the tissue, and the HIV-1 was X4 virus. Therefore, these data suggest that the HIV-1 might be detected from lymphoma cells, not from contaminated T cells or macrophages, and integrate into more than 20% of the lymphoma cells.

3.4. Promoter activity and methylation of HIV-1 3′LTR

LTRs of HIV-1 usually have a promoter activity in HIV-1-infected T cells and macrophages [18]. To investigate if the HIV-1 3′LTR contained a functional promoter, we constructed a plasmid containing the patient's HIV-1 3′LTR or upstream intron sequence of STAT3 before a luciferase reporter gene. Transfection of the plasmid to HeLa cells revealed that the sequence of 3′LTR derived from the patient had significant promoter activity at a similar level to that of 3′LTR in HIV-1 NL4-3, but the upstream intron sequence of STAT3 did not (Fig. 4A). 3′LTR was a stronger promoter than the STAT3 promoter derived from the patient. Cotransfection with a plasmid expressing HIV-1-Tat enhanced the activity of the patient's 3′LTR 31-fold, whereas the activity of the STAT3 promoter was not enhanced. These data suggest that the HIV-1 3′LTR contains promoter activity. It is known that DNA CpG methylation inactivates retroviral promoter including HIV-1 LTR [12,19]. However, a bisulfite genomic sequence revealed that the fragment of HIV-1 3′LTR did not have any CpG or non-CpG methylation in the DNA extracted from the lymphoma (Fig. 4B,C). These data suggest that methylation might not reduce or inhibit the transcriptional activity of HIV-1 3′LTR in the HIV-1-integrated lymphoma cells.

3.5. Expression of STAT3 in the HIV-1-integrated lymphoma

We investigated expression of STAT3 in the case of HIV-1-integrated lymphoma. Immunohistochemistry demonstrated a high level of STAT3 expression predominantly in the nuclei

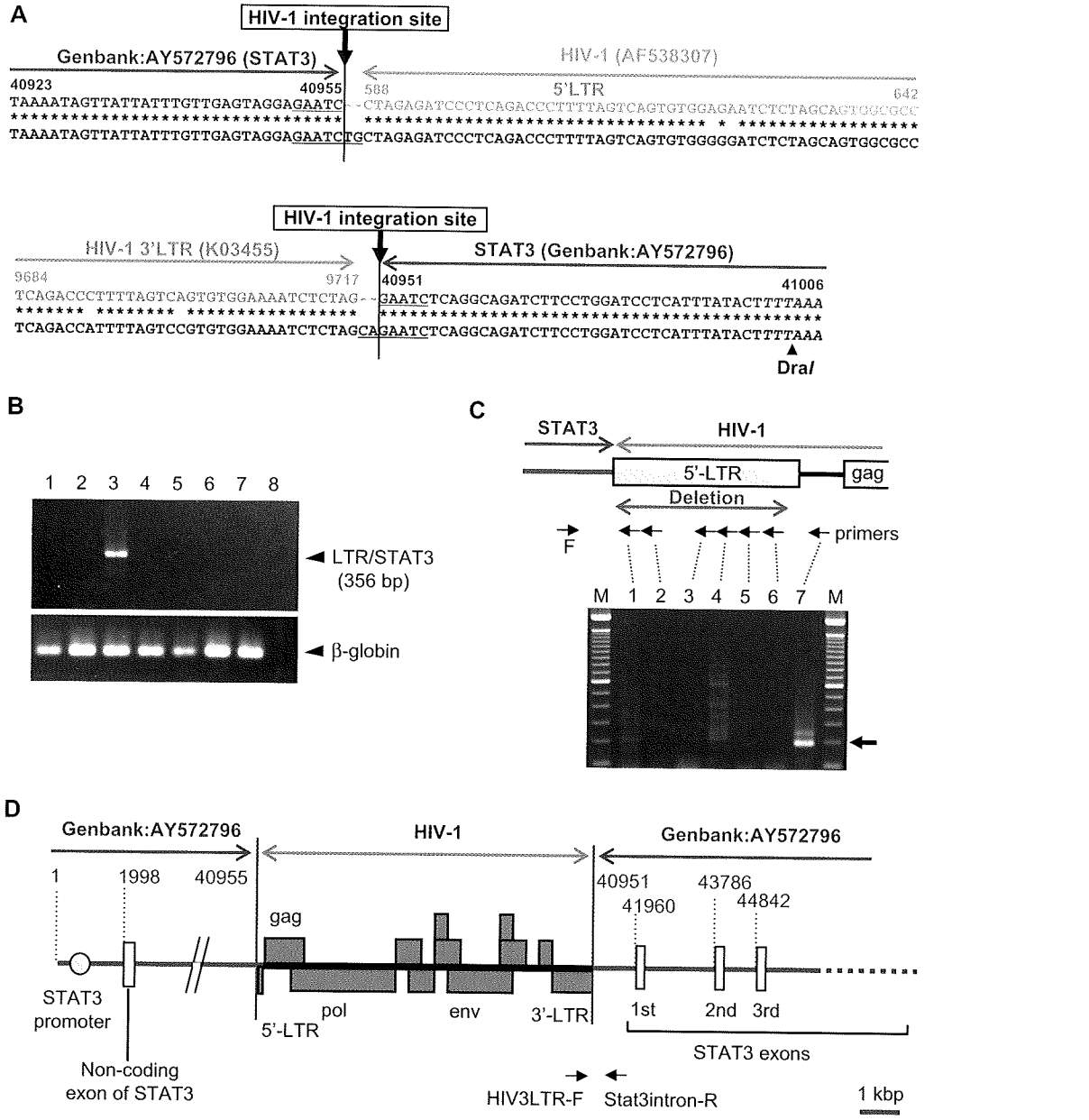

Fig. 2. Identification of HIV-1 integration site in the lymphoma cells with genome walking. (A) Sequence of the HIV-1 5′-LTR (upper panel) and 3′-LTR (lower panel) insertion site in the lymphoma genome. Whole sequences of PCR products are registered as GenBank DQ355432 (5′-LTR, 190 bp) and DQ117603 (3′-LTR, 1.5 kbp), respectively. The sequence of the lymphoma genome is shown in the lower line in black letters. The upper colored line indicates the HIV-1 LTR sequence (blue, GenBank K03455 or AF538307) and STAT3 genomic sequence (violet, GenBank AY572796). HIV-1 intervening sequence between 5′LTR and gag is indicated by green. Duplication of the cellular 5 bp (GAATC) and additional dinucleotides (TG in 5′-LTR and CA in 3′-LTR) by HIV-1 integrase are underlined. *DraI* site is indicated by italics. (B) PCR for the junction region of 3′LTR and STAT3 gene using HIV3LTR-F and Stat3intron-R primers (see Fig. 3D). 1, PBMCs from a healthy donor; 2, HIV-1-positive Molt4 cell line; 3, lymphoma cells with HIV-1integration; 4, KS lesion from the patient; 5, AIDS-related lymphoma from an unrelated patient; 6, lymphoma from a non-HIV-1infected patient; 7, BCBL-1 (KSHV-positive B cell line); 8, No DNA. The lower panel shows the results of an internal control (β-globin gene). (C) PCR of genomic DNA with a STAT3-intron forward primer (F in this figure, Stat3-intronF2) in combination with 5′ LTR reverse primers (lanes 1–6, 55R, 78R, 348R, 495R, 563R and 612R), and a reverse primer positioning between 5′LTR and gag (lane 7, 676R). The upper panel shows the positions of these primers. A 188 bp product was identified when the 676R primer was used with the STAT3 intron primer (lane 7). If the 5′LTR was intact, the predicted size of this amplicon would have been 777 bp. (D) Map of the defective HIV-1 insertion site in the STAT3 gene. Violet numbers indicate the number in GenBank AY572796 (STAT3). Blue boxes are HIV-1 genomes.

of the HIV-1-integrated lymphoma cells (Fig. 4D). To know the phosphorylation status of STAT3, we immunostained the slide using an anti-pSTAT3 (Tyr-705) antibody as a primary antibody. However, any signal was not found in the lymphoma cells (data not shown). We also examined STAT3 expression in 24 cases of lymphoma, including nine cases of AIDS-related lymphoma and 15 of non-AIDS-related lymphoma, normal tonsilar tissues and lymph nodes derived from unrelated patients. The nine cases of AIDS-related lymphoma contained seven of EBV-positive diffuse large B cell lymphoma

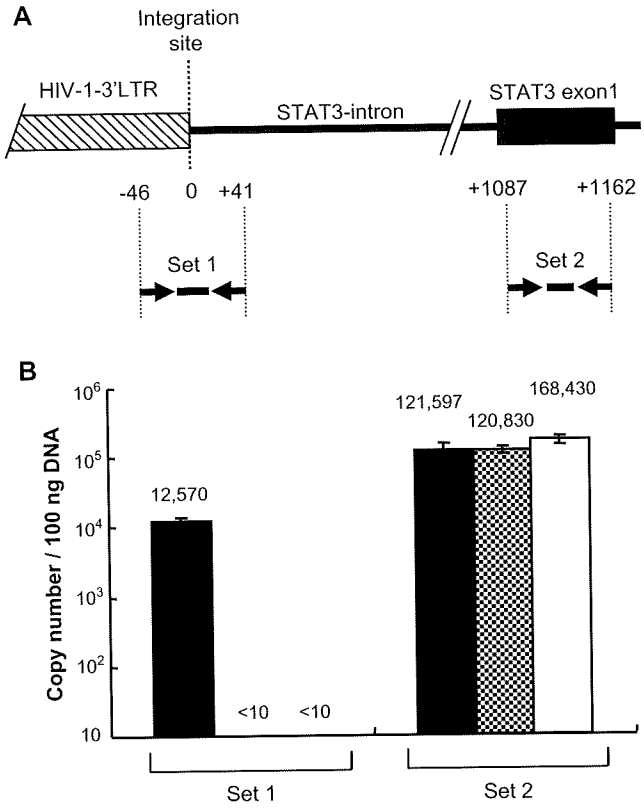

Fig. 3. Quantitative analysis of genes for HIV-1 integration site. (A) Probe-primer sets for real time PCR. The top line with boxes is a genome map around HIV-1 integration site of HIV-1 3′LTR. Numbers with plus and minus under the genome map indicate distances (bp) from the integration site. Arrows and heavy lines are probe-primer sets of real time PCR. (B) Copy numbers of HIV-1 integration site and STAT3 gene. Black, gray and white bars indicate mean copy number per 100 ng DNA of this case, HIV-1-positive Molt4 cell line, and TY-1 (HIV-1-negative, KSHV-positive B cell line), respectively. Copy numbers per 100 ng DNA are indicated on the top of each bar. Error bars indicate standard errors of triplicate samples.

(DLBCL), and two cases of Hodgkin's disease. The 15 cases of non-AIDS-related lymphoma contained 12 EBV-positive or EBV-negative DLBCL and three cases of Hodgkin's disease. Immunohistochemistry revealed that several cases of AIDS-related lymphoma and one of HIV-unrelated lymphoma expressed STAT3 predominantly in the cytoplasm (Fig. 4E); however, no case expressed STAT3 predominantly in the nucleus (Table 1). STAT3 expression was not found, or was weak, in other cases examined (Fig. 4F). These data suggest that the integration of HIV-1 induced high expression of STAT3 in the lymphoma cells of the patient.

3.6. Transfection of STAT3 expression plasmid to primary B cells in vitro

To investigate if expression of STAT3 induces cell growth, we constructed an expression plasmid for STAT3 and transfected the plasmid to B cells. At first, to confirm expression of STAT3 by Nucleofector transfection, His-tagged STAT3 was expressed in TY-1, a KSHV-positive B cell line. Immunofluorescence assay using anti-STAT3 and anti-6x His antibodies revealed that transfection efficiency to lymphocytes was 30–40% in this experiment (Fig. 5A). Addition of IL-6 to culture medium of transfected TY-1 altered the localization of STAT3 from the cytoplasm to the nucleus, suggesting that the transfected STAT3 reacted with IL-6 stimulation (Fig. 5B). Then, we investigated the proliferation of STAT3-transfected primary B cells. Cell proliferation assay after 48 h transfection showed that the proliferation of STAT3-transfected primary B cells were slightly higher than that of vector-transfected primary B cells (Fig. 5C, Mann–Whitney test, $p < 0.01$). However, 4 days after transfection, the difference was not statistically significant (data not shown). The transfection of STAT3 to B cells was repeated 4 times with similar results. These data suggested that transfection of STAT3 might induce a transient proliferation in the primary B cells in vitro.

4. Discussion

In the present study, we present a case of AIDS-related B cell lymphoma with HIV-1 integration. HIV-1 with defective 5′LTR integrated into the upstream region of the first STAT3 coding exon. The 3′ LTR had strong promoter activity, resulting in increased expression of STAT3 in the nuclei of lymphoma cells. This is the first case report describing dysregulation of STAT3 by HIV-1 integration, resulting in B cell lymphoma development.

STAT3 is an important molecule for IL-6-type cytokines that signal and stimulate proliferation and terminal differentiation of B cells [20]. STAT3 also plays some oncogenic roles. Activated and phosphorylated STAT3 has been observed in a variety of experimental and numerous human malignancies [21–23]. A recent study reveals that high expression of unphosphorylated STAT3 results in up-regulation of oncogenes, suggesting that overexpression of either form of STAT3, phosphorylated and unphosphorylated, might induce cancer [24]. Although we failed to detect phosphorylated STAT3, high expression of STAT3 in the nucleus implies that activated STAT3 may bind to DNA and activate some genes constitutively. Alternatively, it implies that overexpression of unphosphorylated STAT3 in the nucleus might induce various oncogenes such as cdc2, cyclin B1 and mras [24]. However, our transfection study of STAT3 resulted in transient cell proliferation in the primary B cells (Fig. 5), suggesting that additional factors other than STAT3 expression might be required for complete transformation of primary B cells. HIV-1 integrated into *c-fes/fps* in other reported cases of AIDS-related lymphoma [6], and it has been demonstrated that *c-fes* activates STAT3 [25]. Thus, STAT3 may play some roles in the lymphomagenesis in the cases of HIV-1-integrated lymphoma.

This case was B cell lymphoma. HIV-1 usually infects and integrates into T cells or macrophages, and it is uncommon for HIV-1 to infect B cells. In the report by other group, HIV-1 provirus was frequently detected in macrophages infiltrating lymphomas, not in lymphoma cells [6]. However, in our case, we concluded that the HIV-1 integration occurred in the lymphoma cells, not in T cells or macrophages infiltrating

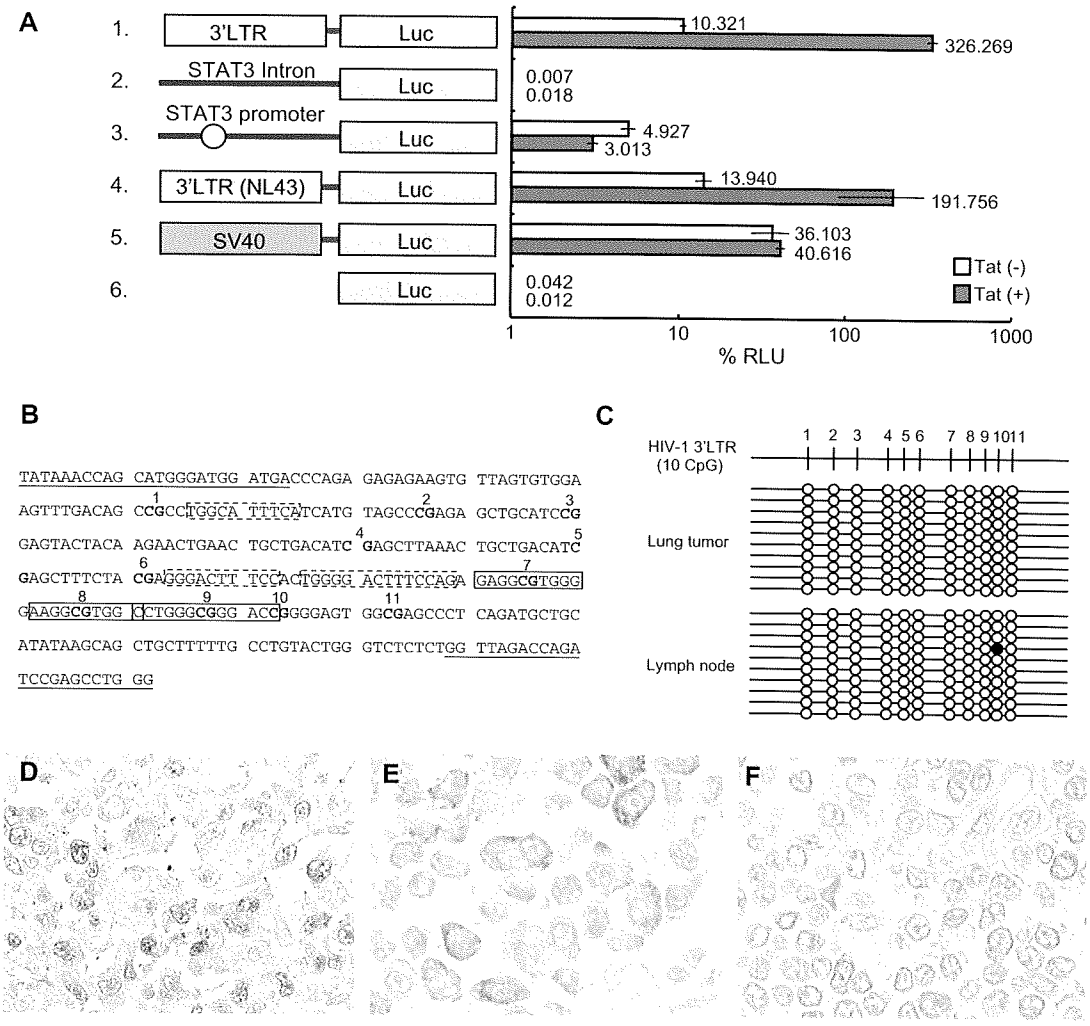

Fig. 4. Promoter activity of HIV-1 3′LTR and STAT3 expression in the lymphoma. (A) Promoter activity of HIV-1 3′LTR by reporter assay. Schematic representation of promoter constructs used in transient transfection assays is shown on the left. Forty-eight hours after transfection, cells were collected and the luciferase activity was measured. The percentage relative luminescence units (RLU) were calculated by dividing firefly activity by renilla activity. Horizontal bars indicate standard deviations of three independent experiments. (B and C) No methylation in a promoter enhancer region of HIV-1 3′LTR in the HIV-1-integrated lymphoma. (B) CpG sites in the promoter enhancer region of 3′LTR of the HIV-1 provirus in the patient with HIV-1-integrated lymphoma (218–529 in GenBank DQ117603). CpG sites are in boldface and numbered from the 5′ end of the LTR (1–11). Nuclear factor-κB and Sp1 sites identified with Motif Search (Kyoto University Bioinfomatics center, Kyoto, Japan, http://motif.genome.jp/) at a 75% cut-off value are indicated by boxes with broken and solid lines, respectively. Sequences used for primers are indicated by underlining. (C) Levels of CpG methylation of the promoter enhancer region of HIV-1 3′LTR in the HIV-1-integrated lymphoma and lymph nodes in the patient. Results of bisulfite genomic sequencing coupled with TA cloning are shown. The methylation status of 10 clones for each sample is presented; methylation of each CpG site is expressed as a filled circle, and unmethylated sites are shown as open circles. Top, schematic description of CpG sites in the 3′LTR of (B). (D–F) Immunohistochemistry of STAT3. The HIV-1-integrated lymphoma cells expressed STAT3 predominantly in the nucleus (D), however, signals of STAT3 were weak and localized in the cytoplasm in the other case of KSHV-positive, AIDS-related lymphoma (E), and were very weak in a case of EBV-positive, AIDS-related lymphoma (F). Original magnification is ×400.

in the lymphoma, because of following reasons: (1) there were few T cells in the lymphoma tissue by immunohistochemistry for CD3 (data not shown); (2) HIV-1 DNA was detected in the lymphoma at a high copy number, that is very rare or none in AIDS-related lymphoma [26]; (3) HIV-1 sequences suggested the possibility of X4 viruses, which leads the integrated HIV-1 sequences are usually not found in the macrophages; (4) some different HIV-1 V3 sequences were identified between the lymphoma and lymph node; and (5) the titer of HIV-1 DNA in the lymphoma were higher than that in the lymph node (Fig. 1G). Then, how did HIV-1 infect B cells in the patient? Although detail mechanism of HIV-1 infection to B cells in this case was still unknown, we presume that KSHV played an important role in HIV-1 infection to B cells. This case of lymphoma was positive for KSHV and EBV by PCR, however, KSHV and EBV did not play a direct role in the oncogenesis of the lymphoma because of the low or absent expression of

Table 1
STAT3 expression in AIDS-related and unrelated lymphoma

STAT3 expression	Nucleus	Cytoplasm	No expression	Total
AIDS-related lymphoma	1*	7	2	10
Non-AIDS-related lymphoma	0	1	14	15

*HIV-integrated lymphoma reported in the present study.

LANA and EBERs. It is possible that KSHV infection might increase susceptibility of B cells expressing CD4 and CXCR4 to infection with the X4 genotype of the HIV-1 [27]. Moreover, it is demonstrated that KSHV-encoded ORF50 protein increases susceptibility of B cells to infection with HIV-1 [28]. Although ORF50, CD4 and CXCR4 were not detected in the lymphoma cells by immunohistochemistry (data not shown), it is possible that KSHV-infected B cells might be infected and integrated by HIV-1 in the early stage of lymphoma development.

Although an intensive study revealed that there were many hot spots of HIV-1 integration [29], the STAT3 gene was not included in the list of hot spots. Thus, the STAT3 gene is a novel target of HIV-1 integration. Since HIV-1 DNA has not been detectable in DNAs extracted from AIDS-related lymphoma cases by Southern blot hybridization, so far [26], HIV-1 integration should be rare in AIDS-related lymphoma. A recent study demonstrates a decrease in EBV-positive lymphoma among patients with AIDS because of introduction of highly active antiretroviral therapy (HAART) [30]. Therefore, novel mechanisms other than oncogenesis by EBV or KSHV may have been involved in the lymphomagenesis of AIDS-related lymphoma recently. There is no report describing a frequency of HIV-1 integration among AIDS related lymphoma. HIV-1 usually infects T cells or macrophages in AIDS patients, however, T cell lymphoma is still rare among AIDS-related lymphoma in the HAART era [30]. In addition, HIV-1 infection to B cells would occur in a very special condition, such as under KSHV infection. Taken together, although the case we described in the present study contained an important scientific phenomenon on STAT3, HIV-1-integrated lymphoma should be very rare among AIDS-related lymphoma.

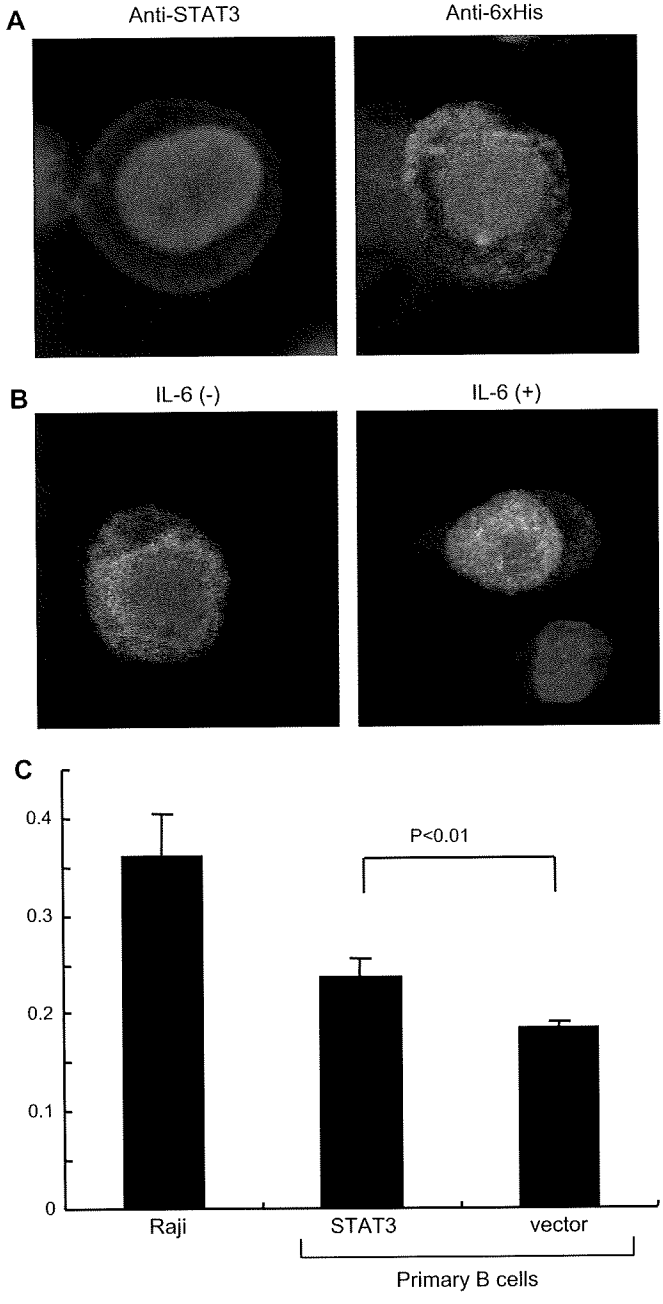

Fig. 5. Transfection of STAT3 into B cells in vitro. (A) STAT3 expression in the STAT3-transfected TY-1, a KSHV-positive B cell line. The cells were transfected with STAT3 expression vector by Nucleofector (Amaxa, Cologne, Germany) using O-06 program. STAT3 expression was detected by anti-STAT3 mouse monoclonal antibody (green in left panel) and anti-6xHis antibody, followed by Alexa 488-conjugated anti-mouse IgG antibody (molecular probe, green in right panel). Red color indicates nuclear counterstaining of propidium iodide. (B) Localization of transfected STAT3 in TY-1. His-tagged STAT3 was detected by anti-6x His antibody in the cytoplasm of B cells (left panel). In the presence of IL-6 (Peprotech, Rocky Hill, NJ, 0.1 ng/ml), transfected STAT3 localizes in the nucleus predominantly (right panel). (C) Cell proliferation assay for STAT3-transfected primary B lymphocytes. Primary B cells were isolated from PBMC. The purity of B cell (CD19+) was >95%. The cells were transfected with STAT3 expression vector expressing STAT3 and CD4 by Nucleofector using U-15 program. Transfection efficiency to primary B cells was around 20%. To increase the proportion of transfected cells, the transfected B cells were separated with CD4 microbeads after 16 h of the transfection (Miltenyl Biotec, Auburn, CA). 48 h after transfection of STAT3 or vector to primary B cells, the proliferation rate was measured with BrdU ELISA (Roche). Raji is an EBV-positive Burkitt lymphoma cell line (untransfected). Numbers in Y-axis indicates absorbance in ELISA. Error bars indicate standard errors of 8 independent experiments.

Acknowledgments

This study was supported by Health and Labor Sciences Research Grants on HIV/AIDS from the Ministry of Health, Labor and Welfare (grants H15-AIDS-005 to H.K.), a Grants-in-Aid for Scientific Research from the Ministry of Education, Culture, Sports, Science and Technology of Japan (grant 19590485 to H.K.), a grant for Research on Health Sciences focusing on Drug Innovation from Japan Health Sciences Foundation (grant SA14831 to H.K.), NIH MO1 RR00096 (to W.N.R.), NIH HL57879 (to M.D.W.), NIH HL 59832 (to M.D.W.), NIH DA022162 (to Y.H.), American Lung Association (to M.D.W.), Japanese Foundation for AIDS Prevention (to Y.H.), Uehara Memorial Foundation (to Y.H.) and the New York University Center for AIDS Research (to Y.H.). The authors declare that they have no competing financial interests.

References

[1] A. Carbone, Emerging pathways in the development of AIDS-related lymphomas, Lancet Oncol. 4 (2003) 22–29.

[2] C. Boshoff, R. Weiss, AIDS-related malignancies, Nat. Rev. Cancer 2 (2002) 373–382.

[3] P.S. Moore, Y. Chang, Kaposi's Sarcoma-Associated Herpesvirus, Lippincott Williams & Wilkins, Philadelphia, 2001.

[4] A. Chadburn, E. Hyjek, S. Mathew, E. Cesarman, J. Said, D.M. Knowles, KSHV-positive solid lymphomas represent an extra-cavitary variant of primary effusion lymphoma, Am. J. Surg. Pathol. 28 (2004) 1401–1416.

[5] S. Hacein-Bey-Abina, C. Von Kalle, M. Schmidt, M.P. McCormack, N. Wulffraat, P. Leboulch, A. Lim, C.S. Osborne, R. Pawliuk, E. Morillon, R. Sorensen, A. Forster, P. Fraser, J.I. Cohen, G. de Saint Basile, I. Alexander, U. Wintergerst, T. Frebourg, A. Aurias, D. Stoppa-Lyonnet, S. Romana, I. Radford-Weiss, F. Gross, F. Valensi, E. Delabesse, E. Macintyre, F. Sigaux, J. Soulier, L.E. Leiva, M. Wissler, C. Prinz, T.H. Rabbitts, F. Le Deist, A. Fischer, M. Cavazzana-Calvo, LMO2-associated clonal T cell proliferation in two patients after gene therapy for SCID-X1, Science 302 (2003) 415–419.

[6] B. Shiramizu, B.G. Herndier, M.S. McGrath, Identification of a common clonal human immunodeficiency virus integration site in human immunodeficiency virus-associated lymphomas, Cancer Res. 54 (1994) 2069–2072.

[7] H. Katano, Y. Sato, T. Kurata, S. Mori, T. Sata, Expression and localization of human herpesvirus 8-encoded proteins in primary effusion lymphoma, Kaposi's sarcoma, and multicentric Castleman's disease, Virology 269 (2000) 335–344.

[8] H. Katano, Y. Sato, T. Kurata, S. Mori, T. Sata, High expression of HHV-8-encoded ORF73 protein in spindle-shaped cells of Kaposi's sarcoma, Am. J. Pathol. 155 (1999) 47–52.

[9] H. Katano, Y. Hoshino, Y. Morishita, T. Nakamura, H. Satoh, A. Iwamoto, B. Herndier, S. Mori, Establishing and characterizing a CD30-positive cell line harboring HHV-8 from a primary effusion lymphoma, J. Med. Virol. 58 (1999) 394–401.

[10] H. Katano, Y. Sato, T. Sata, Expression of p53 and human herpesvirus 8 (HHV-8)-encoded latency-associated nuclear antigen (LANA) with inhibition of apoptosis in HHV-8-associated malignancies, Cancer 92 (2001) 3076–3084.

[11] Y. Asahi-Ozaki, Y. Sato, T. Kanno, T. Sata, H. Katano, Quantitative analysis of Kaposi sarcoma-associated herpesvirus (KSHV) in KSHV-associated diseases, J. Infect. Dis. 193 (2006) 773–782.

[12] T. Koiwa, A. Hamano-Usami, T. Ishida, A. Okayama, K. Yamaguchi, S. Kamihira, T. Watanabe, 5′-long terminal repeat-selective CpG methylation of latent human T-cell leukemia virus type 1 provirus in vitro and in vivo, J. Virol. 76 (2002) 9389–9397.

[13] Y. Hoshino, K. Nakata, S. Hoshino, Y. Honda, D.B. Tse, T. Shioda, W.N. Rom, M. Weiden, Maximal HIV-1 replication in alveolar macrophages during tuberculosis requires both lymphocyte contact and cytokines, J. Exp. Med. 195 (2002) 495–505.

[14] H. Katano, T. Suda, Y. Morishita, K. Yamamoto, Y. Hoshino, K. Nakamura, N. Tachikawa, T. Sata, H. Hamaguchi, A. Iwamoto, S. Mori, Human herpesvirus 8-associated solid lymphomas that occur in AIDS patients take anaplastic large cell morphology, Mod. Pathol. 13 (2000) 77–85.

[15] Y. Hoshino, D.B. Tse, G. Rochford, S. Prabhakar, S. Hoshino, N. Chitkara, K. Kuwabara, E. Ching, B. Raju, J.A. Gold, W. Borkowsky, W.N. Rom, R. Pine, M. Weiden, *Mycobacterium tuberculosis*-induced CXCR4 and chemokine expression leads to preferential X4 HIV-1 replication in human macrophages, J. Immunol. 172 (2004) 6251–6258.

[16] P.O. Brown, B. Bowerman, H.E. Varmus, J.M. Bishop, Retroviral integration: structure of the initial covalent product and its precursor, and a role for the viral IN protein, Proc. Natl. Acad. Sci. USA 86 (1989) 2525–2529.

[17] T. Fujiwara, K. Mizuuchi, Retroviral DNA integration: structure of an integration intermediate, Cell 54 (1988) 497–504.

[18] Y. Hoshino, S. Hoshino, J.A. Gold, B. Raju, S. Prabhakar, R. Pine, W.N. Rom, K. Nakata, M. Weiden, Mechanisms of PMN-mediated induction of HIV-1 replication in macrophages during pulmonary tuberculosis, J. Infect. Dis. (2007) 1303–1310.

[19] D.P. Bednarik, J.A. Cook, P.M. Pitha, Inactivation of the HIV LTR by DNA CpG methylation: evidence for a role in latency, Embo J 9 (1990) 1157–1164.

[20] P.C. Heinrich, I. Behrmann, G. Muller-Newen, F. Schaper, L. Graeve, Interleukin-6-type cytokine signalling through the gp130/Jak/STAT pathway, Biochem. J. 334 (Pt 2) (1998) 297–314.

[21] J.F. Bromberg, M.H. Wrzeszczynska, G. Devgan, Y. Zhao, R.G. Pestell, C. Albanese, J.E. Darnell Jr., Stat3 as an oncogene, Cell 98 (1999) 295–303.

[22] R. Catlett-Falcone, W.S. Dalton, R. Jove, STAT proteins as novel targets for cancer therapy. Signal transducer an activator of transcription, Curr. Opin. Oncol. 11 (1999) 490–496.

[23] T.S. Lin, S. Mahajan, D.A. Frank, STAT signaling in the pathogenesis and treatment of leukemias, Oncogene 19 (2000) 2496–2504.

[24] J. Yang, M. Chatterjee-Kishore, S.M. Staugaitis, H. Nguyen, K. Schlessinger, D.E. Levy, G.R. Stark, Novel roles of unphosphorylated STAT3 in oncogenesis and transcriptional regulation, Cancer Res. 65 (2005) 939–947.

[25] K.L. Nelson, J.A. Rogers, T.L. Bowman, R. Jove, T.E. Smithgall, Activation of STAT3 by the c-Fes protein-tyrosine kinase, J. Biol. Chem. 273 (1998) 7072–7077.

[26] P.G. Pelicci, D.M. Knowles 2nd, Z.A. Arlin, R. Wieczorek, P. Luciw, D. Dina, C. Basilico, R. Dalla-Favera, Multiple monoclonal B cell expansions and c-myc oncogene rearrangements in acquired immune deficiency syndrome-related lymphoproliferative disorders. Implications for lymphomagenesis, J. Exp. Med. 164 (1986) 2049–2060.

[27] R. Merat, A. Amara, C. Lebbe, H. de The, P. Morel, A. Saib, HIV-1 infection of primary effusion lymphoma cell line triggers Kaposi's sarcoma-associated herpesvirus (KSHV) reactivation, Int. J. Cancer 97 (2002) 791–795.

[28] E. Caselli, M. Galvan, F. Santoni, A. Rotola, A. Caruso, E. Cassai, D.D. Luca, Human herpesvirus-8 (Kaposi's sarcoma-associated virus) ORF50 increases in vitro cell susceptibility to human immunodeficiency virus type 1 infection, J. Gen. Virol. 84 (2003) 1123–1131.

[29] A.R. Schroder, P. Shinn, H. Chen, C. Berry, J.R. Ecker, F. Bushman, HIV-1 integration in the human genome favors active genes and local hotspots, Cell 110 (2002) 521–529.

[30] T. Hishima, N. Oyaizu, T. Fujii, N. Tachikawa, A. Ajisawa, M. Negishi, T. Nakamura, A. Iwamoto, Y. Hayashi, D. Matsubara, Y. Sasao, S. Kimura, Y. Kikuchi, K. Teruya, A. Yasuoka, S. Oka, K. Saito, S. Mori, N. Funata, T. Sata, H. Katano, Decrease in Epstein–Barr virus-positive AIDS-related lymphoma in the era of highly active antiretroviral therapy, Microbes Infect. 8 (2006) 1301–1307.

Journal of Medical Virology 82:400–406 (2010)

Genotypic and Clinicopathological Characterization of Kaposi's Sarcoma-Associated Herpesvirus Infection in Japan

Takayuki Kanno, Yuko Sato, Tomoyuki Nakamura, Kouta Sakamoto, Tetsutaro Sata, and Harutaka Katano*

Department of Pathology, National Institute of Infectious Diseases, Shinjuku, Tokyo, Japan

Kaposi's sarcoma-associated herpesvirus (KSHV) is related causally to Kaposi's sarcoma, primary effusion lymphoma, and a subset of cases of multicentric Castleman's disease. As the numbers of acquired immunodeficiency syndrome (AIDS) patients have increased, KSHV-associated diseases have also increased in Japan. Sporadic cases of classic Kaposi's sarcoma have also been reported in Japan. In the present study, the clinicopathological characteristics of 75 samples, comprising 68 cases of Kaposi's sarcoma, 5 cases of primary effusion lymphoma, and 5 cases of multicentric Castleman's disease were investigated. All of these cases were positive for KSHV by immunohistochemistry or PCR analysis. All fifty-two of the AIDS-associated Kaposi's sarcoma cases were males, whereas 7 of the 13 non-AIDS-associated Kaposi's sarcoma cases were females. The mean age of patients with AIDS-associated Kaposi's sarcoma or primary effusion lymphoma was 46 years, whereas the mean age of patients with non-AIDS-associated Kaposi's sarcoma or primary effusion lymphoma was 71.8 and 97.5, respectively. KSHV genotypes were determined based on the sequence of variable region 1 in the *K1* gene. Genotypes A and C of KSHV were detected in both AIDS- and non-AIDS-associated Kaposi's sarcoma. Genotype A was detected more frequently in AIDS-associated cases than non-AIDS-associated cases, suggesting that genotype C is broadly distributed in Japan, and genotype A spreads among AIDS patients. Genotype D was detected only in non-AIDS-associated Kaposi's sarcoma. These data confirmed the difference between AIDS- and non-AIDS-associated KSHV diseases with regard to age of onset, gender, and genotypes in Japan. ***J. Med. Virol. 82:400–406, 2010.*** © 2010 Wiley-Liss, Inc.

KEY WORDS: Kaposi's sarcoma; Kaposi's sarcoma-associated herpesvirus; AIDS; genotype

INTRODUCTION

Kaposi's sarcoma-associated herpesvirus (KSHV, also known as human herpesvirus-8, HHV-8) was identified from a Kaposi's sarcoma (KS) specimen by representational difference analysis in 1994 [Chang et al., 1994]. KSHV has been detected in KS, primary effusion lymphoma (PEL) and a subset of multicentric Castleman's disease (MCD) cases [Moore and Chang, 2001]. KS was first described in 1872 by Moriz Kaposi, a Hungarian dermatologist, as an idiopathic, multipigmented sarcoma of the skin [Kaposi, 1872]. KS is classified into four types: classic, endemic, iatrogenic, and acquired immunodeficiency syndrome (AIDS)-associated KS (AIDS-KS) [Antman and Chang, 2000]. Classic KS affects typically elderly men in Mediterranean littoral, endemic KS affects typically people in Africa, iatrogenic KS affects most commonly organ-transplant recipients receiving immunosuppressive therapy and AIDS-KS is mainly associated with homosexual men infected with human immunodeficiency virus (HIV). In Japan, KS was a very rare condition prior to 1980 [Fujii et al., 1986]. A few patients with adult

The authors declare no conflict of interest.

Grant sponsor: Japanese Health Sciences Foundation (Research on the Publicly Essential Drugs and Medical Devices, partial support to TK, TS, and HK); Grant number: SAA4832; Grant sponsor: Ministry of Health, Labor and Welfare (Health and Labor Sciences Research Grants on Measures for HIV/AIDS to HK); Grant number: H21-AIDS-Ippan-006; Grant sponsor: Ministry of Health, Labor and Welfare (Intractable Diseases to TS); Grant number: H20-Nanchi-Ippan-035; Grant sponsor: Ministry of Health, Labor and Welfare (Emerging and Re-emerging Infectious Diseases to TS and HK); Grant number: H20-Shinko-Ippan-006; Grant sponsor: Ministry of Education, Culture, Sports, Science and Technology of Japan (Grant-in-Aid for Scientific Research to HK); Grant number: 21590520.

*Correspondence to: Harutaka Katano, DDS, Department of Pathology, National Institute of Infectious Diseases, 1-23-1 Toyama, Shinjuku, Tokyo 162-8640, Japan.
E-mail: katano@nih.go.jp

Accepted 17 October 2009

DOI 10.1002/jmv.21715

Published online in Wiley InterScience (www.interscience.wiley.com)

T-cell leukemia were described who had developed KS, from the Kyushu region and the southern island of Okinawa, but very few classic cases of KS were reported from other areas of Japan [Kamada et al., 1992]. After 1980, cases of AIDS-KS increased dramatically in Japan because of the rapid spread of AIDS. The introduction of highly active anti-retroviral therapy (HAART) reduced the number of KS cases in Western countries [Jones et al., 1999]. However, KS cases still increased in Japan after 2000 because of the dissemination of HIV infection within the homosexual male community. As well as AIDS-KS, other KSHV-associated diseases, such as AIDS-PEL and AIDS-MCD, also increased during the past 10 years in Japan [Katano et al., 1999a; Hasegawa et al., 2004; Abe et al., 2006]. Therefore, to prevent the spread of AIDS-KS, it is important to determine the clinicopathological features of KSHV-associated diseases in Japan. To date, reports describing the clinicopathological features of Japanese AIDS-KS have all involved only small sample sizes [Fujii et al., 1986; Kamada et al., 1992; Kondo et al., 2000; Yamada et al., 2000; Meng et al., 2001; Sato-Matsumura et al., 2001; Kamiyama et al., 2004; Minoda et al., 2006; Yoshii et al., 2006; Ueno et al., 2007].

The association of KSHV infection with KS pathogenesis has already been well investigated. A latency-associated nuclear antigen 1 (LANA-1) encoded by KSHV is detected in almost all KS cells, indicating that KS cells are infected with KSHV [Dupin et al., 1999; Katano et al., 1999b]. The genome of KSHV is a double-stranded linear DNA of about 170 kbp, flanked by GC-rich terminal repeats [Russo et al., 1996]. The *K1* gene in KSHV contains highly variable regions 1 and 2 (VR1, VR2) and phylogenetic analysis of the *K1* gene classified KSHV into genotypes A–F [Zong et al., 1997, 1999; Meng et al., 1999; Hayward and Zong, 2007]. These genotypes are differently distributed throughout the world: KSHV genotype A is predominant in North America, B in Africa, C in Eurasia and the Mediterranean, D in the Pacific islands, E in Brazilian Amerindians, and F in the Ugandan Bantu tribe [Zong et al., 1999; Biggar et al., 2000; Kajumbula et al., 2006]. Previous studies involving a small number of cases detected genotypes C and A in cases of KS, and genotype D in some cases of classic KS in Japan [Meng et al., 2001; Kamiyama et al., 2004]. However, it is unknown whether these genotypes are associated with any of the clinical features or pathogenesis of KS or other diseases.

In the present study, the clinicopathological features and genotypes of KSHV-associated diseases were investigated in 75 samples originating from all over Japan. The aim was to determine the characteristics of KSHV-associated diseases in Japan.

MATERIALS AND METHODS

Tissue Specimens

Studies using human tissue were performed with the approval of the Institutional Review Board of the National Institute of Infectious Diseases (Approval No. 158). Seventy-five cases of KSHV-associated disease were filed in the Department of Pathology, National Institute of Infectious Diseases, Japan, from 1995 to April 2009 as consultation cases. They include 68 KS cases, 5 PEL cases, and 5 MCD cases. Two MCD patients and a PEL patient had KS lesions. Frozen tissue samples were available for 21 of these cases. For some other cases, only formalin-fixed paraffin-embedded tissue sections were available. The samples were sent from all over Japan, from the northern island of Hokkaido to Okinawa, the southern island of Japan.

Histological Grading and Immunohistochemistry

Paraffin sections were hematoxylin and eosin stained and subjected to immunohistochemical staining to detect LANA-1, as described previously [Katano et al., 1999b]. Samples were categorized into three clinical stages of KS (patchy, plaque, or nodular stage) according to the clinical data and the histological findings.

Preparation of DNA

Total DNA was extracted from fresh-frozen clinical materials or formalin-fixed paraffin-embedded sections as described previously [Asahi-Ozaki et al., 2006]. For the isolation of DNA from formalin-fixed paraffin-embedded biopsies, three or four 5 μm-sections were placed into sterile eppendorf tubes, deparaffinized with xylene, digested with proteinase K, then extracted using the phenol/chloroform method. For fresh-frozen samples, DNA was extracted using the DNeasy Blood & Tissue kit according to the manufacturer's protocol (Qiagen GmbH, Hilden, Germany).

PCR Amplification and DNA Sequencing

A 160 bp fragment containing VR1 of the *K1* gene was amplified by PCR from DNA samples as described previously [Dilnur et al., 2001]. The primer set used was as follows: forward primer 5′-TTG CCA ATA TCC TGG TAT TGC-3′; reverse primer 5′-CAA GGT TTG TAA GAC AGG TTG-3′. PCR amplification was carried out at 94°C for 2 min (one cycle); 94°C for 1 min, 58°C for 1 min, and 72°C for 2 min (35 cycles); and 72°C for 5 min (one cycle) using the GeneAmp PCR System 9700 (Applied Biosystems, Foster City, CA). PCR products were purified using the QIAquick PCR purification kit (Qiagen), followed by direct sequencing with an ABI sequencer 3130 (Applied Biosystems) using a Big-Dye terminator ready reaction kit (Applied Biosystems) according to the manufacturer's instructions.

Phylogenetic Tree Analysis

Nucleotide sequences, excluding primer sequences, were multiple aligned with CLUSTAL W version 1.83 [Jeanmougin et al., 1998], and a phylogenetic tree was constructed using the neighbor-joining-plot method and Genetyx software (Genetyx, Tokyo, Japan). In addition

to our samples, 20 previously reported *K1* gene sequences were obtained from the GenBank database and used as reference sequences for comparison [Dilnur et al., 2001]. The genotypes of KSHV samples and the GenBank accession numbers of the reference strains are as follows: BCBL-R (genotype A, accession no. AF133038), BCBL-B (A, AF133039), 431KAP (B, AF133040), ASM72 (C, AF133041), BC2 (C, AF133042), TKS10 (D, AF133043), ZKS3 (D, AF133044), US3 (A, AF151688), Ug3 (A, AF151690), US6 (C, AF151686), Au1 (D, AF151687), Ug1 (B, AF151689), 78/48 (C, AF201851), 75/10T (A, AF201848), 80/56 (A, AF2-1853), KS-F (C, U93872), Tupi-1 (E, AF220292), Tupi-2 (AF220293), Wagu128 (E, AY940426), and BCBL-1 (A, U86667) [Meng et al., 1999; Zong et al., 1999; Lacoste et al., 2000; Kazanji et al., 2005]. BCBL-R was used as a consensus sequence.

GenBank Accession Numbers

GenBank accession numbers of Japanese KSHV sequences are AF278837 (J1), AF278842 (J2), AF278847–AF278849 (J3–J5), AF278850–AF278852 (J7–J9), AF278838 (J14), AF278839 (J16), AF278840 (J17), AF278841 (J19), AF278843 (J21), AF278844–AF278846 (J24–J26), and GQ848990–GQ849006 (J27–J43).

Statistical Analysis

Analysis of statistical significance was carried out using the Chi-squared test or Fisher's extract for bivariate tabular analysis and the Mann–Whitney test for comparison of two independent groups of sampled data.

RESULTS

Clinical and Pathological Characteristics of KS in Japan

Table I provides a summary of the clinical data. All of the cases were positive for LANA-1 by immunohistochemistry. The 68 pathological samples of KS were taken from various anatomical sites: the skin (84%), the gastrointestinal tract (7%), the lymph node (4%), the lungs (1%), the oral cavity (1%), and the conjunctive (1%) (Fig. 1A). Non-AIDS-KS cases were all presented in the skin. Among the 68 KS cases, 52 were AIDS-KS (76.4%) and 13 were non-AIDS-KS (19.1%). HIV-1 seropositive data were not available for three KS cases (4.4%). AIDS-KS cases were all from male patients with a mean age of 45.8 years (range: 23–82). By contrast, only six non-AIDS-KS cases were male (46%) and the proportion of female in non-AIDS-KS cases was high (54%). The mean age of non-AIDS-KS cases was 71.8 years (range: 52–87), which was statistically higher than that of AIDS-KS cases (Mann–Whitney test, $P < 0.01$). In addition, the mean age of non-AIDS-associated PEL cases was 97.5 years (range: 94–101), indicating occurrence of PEL in predominantly very elderly patients. Among the non-AIDS-KS cases, nine cases were regarded as classic KS and four cases were iatrogenic KS in immunosuppressed patients. Seven out of 13 non-AIDS-KS cases were in females, including 4 cases of iatrogenic KS. Histologically, the skin lesions of KS were categorized into stages: patchy (27%), plaque (36%), and nodular (34%) (Fig. 1B,C). Among the 13 non-AIDS-KS lesions, 6 lesions (46.2%) were at the plaque stage. However, AIDS-KS lesions represented all three stages, patchy, plaque, and nodular, almost equally. No histological difference was found between AIDS-KS and non-AIDS-KS.

Phylogenetic Tree Analysis of VR1 of the *K1* Gene From KSHV Genotypes

KSHV genotypes were determined in 33 cases based on the sequence of VR1 in the *K1* gene [Meng et al., 1999; Zong et al., 1999]. Thirty strains were obtained from KS samples, three from each of the PEL and MCD samples (Fig. 2A). Sixteen strains (J1–J5, J7–J9, J14, J16, J17, J19, J21, and J24–J26) have been described previously (14 KS, one PEL and one MCD case) [Meng et al., 2001]. Construction of a phylogenetic tree revealed that the Japanese cases were categorized into genotypes A, C, and D (Fig. 2B). Genotypes A and C were observed in the AIDS-KS subjects, whereas genotypes A, C, and D were observed in non-AIDS-KS subjects (Fig. 3A). Thus, genotype D was observed only in non-AIDS-KS subjects. All three cases of PEL, including one case of non-AIDS-PEL, were genotype C. Two genotype C and one genotype A sequences were detected in three cases of AIDS-MCD. Genotype A was detected more frequently

TABLE I. Summary of the Clinical Data of All Disease Cases Used in This Study

	n	Mean age	Age range	No. of males (%)	HIV(+)
KS	**68**	**50.7**	**23–87**	**61 (89.7%)**	**52/65 (80.0%)**
AIDS-KS	52	45.8	23–82	52 (100%)	—
Non-AIDS-KS	13	71.8	52–87	6 (46.1%)	—
Unknown	3	46.0	33–53	3 (100%)	—
PEL	**5***	**64.0**	**42–101**	**5* (100%)**	**3*/5 (60%)**
AIDS-PEL	3*	45.5	42–49	3* (100%)	—
Non-AIDS-PEL	2	97.5	94–101	2 (100%)	—
AIDS-MCD	**5****	**38.8**	**27–56**	**5** (100%)**	**5**/5 (100%)**
All	75	51.2	23–101	68 (90.7%)	57/72 (79.2%)

*Including one case having KS. **Including two cases having KS. Bold indicates large categories.

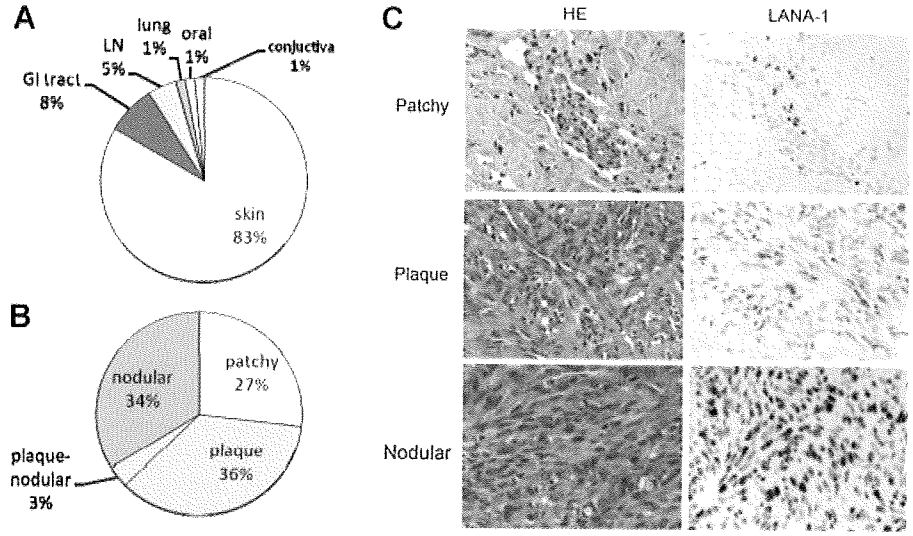

Fig. 1. Site and histology of Japanese Kaposi's sarcoma (KS) cases. Pie charts indicating (**A**) the site of KS and (**B**) the histological stage of KS in the skin, in the cases studied. GI: gastrointestinal, LN: lymph node. **C**: Hematoxylin and eosin (HE) staining (left) and latency-associated nuclear antigen 1 (LANA-1) immunohistochemistry (right) of patchy stage (upper), plaque (middle), and nodular stage (lower) of KS.

in AIDS-associated cases than non-AIDS-associated cases, but the difference was not statistically significant ($P = 0.28$, Chi-square test with Yate's correction) (Fig. 3B). Genotype C was common in both groups. The mean ages associated with genotypes A, C, and D were 48, 56, and 77, respectively. Genotype D was detected in more elderly patients than genotypes A and C ($P < 0.05$, Mann–Whitney test). These data indicated that genotype D was associated with non-AIDS-associated cases, not with AIDS-associated cases. The findings also suggest that genotype C is broadly distributed in Japan, and genotype A spreads among AIDS patients. There was no detectable histological difference among genotypes.

DISCUSSION

In this study, the clinicopathological features and genotypes of Japanese cases of KSHV-associated diseases were demonstrated. These data confirmed that non-AIDS-KSHV-associated diseases occurred predominantly in elderly patients. Genotype analyses suggested the broad distribution of genotype C, association of genotype D with non-AIDS-KS and spread of genotype A among AIDS patients in Japan.

There were few reports describing KS in Japan before 1986, and only 14 cases of classic KS were reported between 1917 and 1982 [Fujii et al., 1986]. A group in Okinawa reported six KS cases, including one adult T-cell leukemia-associated and two AIDS-associated cases in 1992 [Kamada et al., 1992]. After the discovery of KSHV in 1994, the association of KSHV infection in Japanese KS cases was proposed [Tachikawa et al., 1996]. Serological assays revealed that the seroprevalence of KSHV was 1.4% among the general population in Japan [Katano et al., 2000]. Almost all patients with AIDS-KS and non-AIDS-KS had serum antibody to KSHV, and 64% of Japanese AIDS patients, infected with HIV via sexual transmission were positive for anti-KSHV antibody [Katano et al., 2000]. KSHV was detected in all KS cases in Japan with positive immunohistochemical results for LANA-1 [Katano et al., 1999b]. Thus, the correlation between KSHV infection and KS pathogenesis has already been demonstrated in many Japanese cases. However, to date clinical information on Japanese KS cases was rarely reported [Fujii et al., 1986; Kamada et al., 1992; Kondo et al., 2000; Yamada et al., 2000; Kamiyama et al., 2004; Minoda et al., 2006; Yoshii et al., 2006; Ueno et al., 2007]. The difference in the mean age of patients affected by AIDS-KS and non-AIDS-KS was demonstrated in the present study. These results may reflect the population of origin for these patients. Several case studies reported that non-AIDS-KS in Japan is associated with immunosuppression, old age, or iatrogenic factors [Kondo et al., 2000; Yamada et al., 2000; Sato-Matsumura et al., 2001; Yoshii et al., 2006]. Regarding AIDS-KS, an epidemiological survey revealed that 70% of newly-HIV-infected individuals were infected via homosexual behavior (AIDS Surveillance Committee Japan, 2008). HAART decreased the incidence of KS in HIV-infected patients, but the increase of HIV-infection in homosexual men resulted in an increase of AIDS-KS cases in Japan. Although it is suggested that KSHV may be spread among homosexual men in Japan, further epidemiological studies on HIV-infected and uninfected males would be required to clarify the association of KSHV infection with the increase of KS in Japan.

KSHV genotypes are determined based on the sequence of VR1 in the *K1* gene sequence of KSHV [Meng et al., 1999; Zong et al., 1999]. Several variable regions were identified in the KSHV genome [Poole

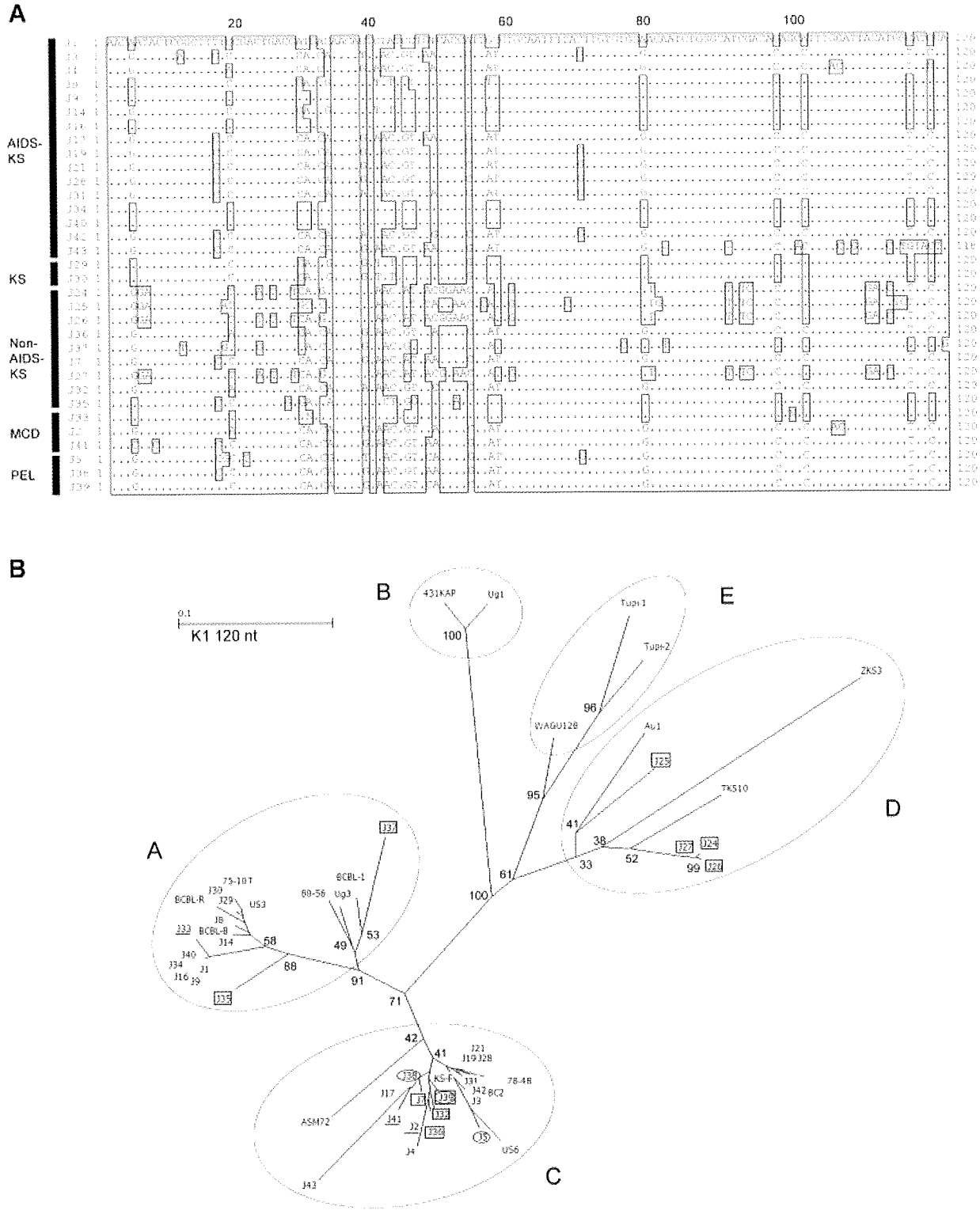

Fig. 2. K1 gene sequences in Japanese cases. **A**: Alignment of K1 gene sequences. One hundred twenty basepair fragments containing VR1 of the *K1* gene are shown. Case J33 had not only MCD, but also KS. HIV-1 seropositive data were not available for J29 and J30 cases. **B**: Radial unrooted phylogenetic tree generated by the NJ method on 120 bp segments of the *K1* gene. The numbers at some nodes (boot strap values) indicate frequencies of occurrence for 100 trees. Scale bar represents 0.1 substitutions per site. Genotypes A–E are indicated by circles. Japanese cases are indicated by J-numbers. J-numbers with boxes are non-AIDS cases of KS or PEL. J5 and J38 are AIDS-PEL cases (circled). J39 is a non-AIDS-PEL case (circled and boxed). J2, J33, and J41 are AIDS-MCD cases (underlined). All other sequences are included for reference. See text.

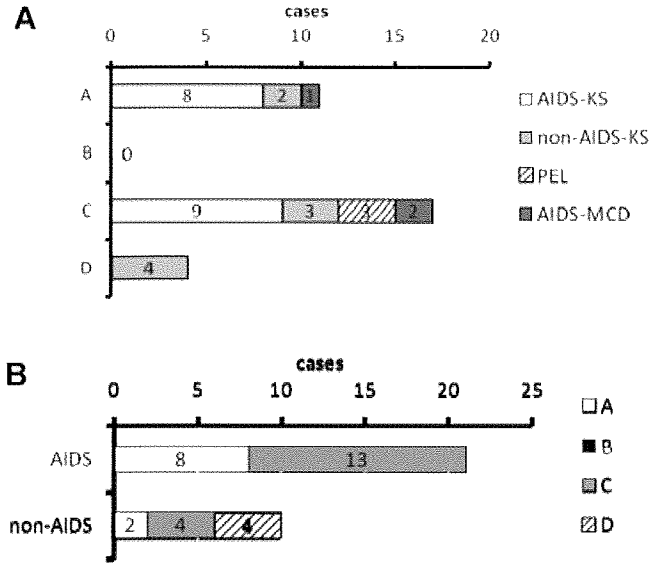

Fig. 3. Graphs indicating the association between: **A**: Kaposi's sarcoma-associated herpesvirus (KSHV) genotypes and diseases (each bar indicates the number of cases). **B**: Genotypes in AIDS-associated and non-AIDS-associated cases.

et al., 1999]. However, since frequent variations were detected in the *K1* gene among strains, the *K1* gene was well investigated and used as a standard for genotype determination [Meng et al., 1999; Zong et al., 1999; Hayward and Zong, 2007]. Genotypes A and C of KSHV are broadly distributed throughout the world. A previous study had already shown that genotype C was predominant not only in Japan, but also in Asian countries, such as Taiwan, Korea, and China [Zong et al., 2002]. Genotype C was detected in Uygur people in Xinjiang, west of China, that was located at the middle point of the Silk Road from Rome to Xian, China [Dilnur et al., 2001]. The virus may therefore have been transmitted via the migration of people from Europe, and the genotype C virus spread in Asian countries. Genotype D, found in the Oceania region, had already been detected in three cases of non-AIDS-KS in Japan in a previous study [Meng et al., 2001]. One additional case of genotype D was found in a non-AIDS-KS case in the present study, supporting the association of genotype D with non-AIDS-KS. Genotype A was detected in both AIDS-KS and non-AIDS-KS cases in the present study. To date, there has been no report of genotype A in non-AIDS-KS cases in Japan. Genotype A was more frequently found in AIDS-KS cases, suggesting that genotype A came from the USA via homosexual activity. However, detection of genotype A in non-AIDS-KS cases at a low rate suggests that genotype A is also a common virus in the general population in Japan, along with genotype C.

PEL and MCD are very rare diseases associated with KSHV infection. A previous study demonstrated that only AIDS-MCD is associated with KSHV infection, not non-AIDS-MCD in Japan [Suda et al., 2001]. All three cases of PEL investigated in this study were genotype C virus, while two genotype C and one genotype A were detected in three cases of MCD. There was no correlation between KSHV genotype and disease, suggesting that any genotype in Japan may induce any type of KSHV-associated disease. Considering 1.4% of KSHV seroprevalence in the general population in Japan, there may be many KSHV-infected individuals without symptoms [Katano et al., 2000]. Although genotype analysis suggests transmission routes of the virus from other countries, further studies using a large number of KSHV-infected patients are needed to clarify the route of KSHV infection among individuals.

REFERENCES

Abe Y, Matsubara D, Gatanaga H, Oka S, Kimura S, Sasao Y, Saitoh K, Fujii T, Sato Y, Sata T, Katano H. 2006. Distinct expression of Kaposi's sarcoma-associated herpesvirus-encoded proteins in Kaposi's sarcoma and multicentric Castleman's disease. Pathol Int 56:617–624.

Antman K, Chang Y. 2000. Kaposi's sarcoma. N Engl J Med 342:1027–1038.

Asahi-Ozaki Y, Sato Y, Kanno T, Sata T, Katano H. 2006. Quantitative analysis of Kaposi sarcoma-associated herpesvirus (KSHV) in KSHV-associated diseases. J Infect Dis 193:773–782.

Biggar RJ, Whitby D, Marshall V, Linhares AC, Black F. 2000. Human herpesvirus 8 in Brazilian Amerindians: A hyperendemic population with a new subtype. J Infect Dis 181:1562–1568.

Chang Y, Cesarman E, Pessin MS, Lee F, Culpepper J, Knowles DM, Moore PS. 1994. Identification of herpesvirus-like DNA sequences in AIDS-associated Kaposi's sarcoma. Science 266:1865–1869.

Dilnur P, Katano H, Wang ZH, Kudo M, Osakabe Y, Sata T, Ebihara Y. 2001. Classic type of Kaposi's sarcoma and human herpesvirus 8 infection in Xinjiang, China. Pathol Int 51:845–852.

Dupin N, Fisher C, Kellam P, Ariad S, Tulliez M, Franck N, van ME, Salmon D, Gorin I, Escande JP, Weiss RA, Alitalo K, Boshoff C. 1999. Distribution of human herpesvirus-8 latently infected cells in Kaposi's sarcoma, multicentric Castleman's disease, and primary effusion lymphoma. Proc Natl Acad Sci USA 96:4546–4551.

Fujii Y, Takayasu S, Yokoyama S, Eizuru Y, Minamishima Y, Enjoji M. 1986. Kaposi's sarcoma in a Korean living in Japan. Review of cases reported in Japanese literature. J Am Acad Dermatol 15:76–82.

Hasegawa H, Katano H, Tanno M, Masuo S, Ae T, Sato Y, Takahashi H, Iwasaki T, Kurata T, Sata T. 2004. BCL-6-positive human herpesvirus 8-associated solid lymphoma arising from liver and spleen as multiple nodular lesions. Leuk Lymphoma 45:2169–2172.

Hayward GS, Zong JC. 2007. Modern evolutionary history of the human KSHV genome. Curr Top Microbiol Immunol 312:1–42.

Jeanmougin F, Thompson JD, Gouy M, Higgins DG, Gibson TJ. 1998. Multiple sequence alignment with Clustal X. Trends Biochem Sci 23:403–405.

Jones JL, Hanson DL, Dworkin MS, Ward JW, Jaffe HW. 1999. Effect of antiretroviral therapy on recent trends in selected cancers among HIV-infected persons. Adult/Adolescent Spectrum of HIV Disease Project Group. J Acquir Immune Defic Syndr 21:S11–S17.

Kajumbula H, Wallace RG, Zong JC, Hokello J, Sussman N, Simms S, Rockwell RF, Pozos R, Hayward GS, Boto W. 2006. Ugandan Kaposi's sarcoma-associated herpesvirus phylogeny: Evidence for cross-ethnic transmission of viral subtypes. Intervirology 49:133–143.

Kamada Y, Iwamasa T, Miyazato M, Sunagawa K, Kunishima N. 1992. Kaposi sarcoma in Okinawa. Cancer 70:861–868.

Kamiyama K, Kinjo T, Chinen K, Iwamasa T, Uezato H, Miyagi JI, Mori N, Yamane N. 2004. Human herpesvirus 8 (HHV8) sequence variations in HHV8 related tumours in Okinawa, a subtropical island in southern Japan. J Clin Pathol 57:529–535.

Kaposi M. 1872. Idiopatiches multiples pigment sarcom der Haut. Arch Dermatol Syphil 4:265–272.

Katano H, Hoshino Y, Morishita Y, Nakamura T, Satoh H, Iwamoto A, Herndier B, Mori S. 1999a. Establishing and characterizing a CD30-positive cell line harboring HHV-8 from a primary effusion lymphoma. J Med Virol 58:394–401.

Katano H, Sato Y, Kurata T, Mori S, Sata T. 1999b. High expression of HHV-8-encoded ORF73 protein in spindle-shaped cells of Kaposi's sarcoma. Am J Pathol 155:47–52.

Katano H, Iwasaki T, Baba N, Terai M, Mori S, Iwamoto A, Kurata T, Sata T. 2000. Identification of antigenic proteins encoded by human herpesvirus 8 and seroprevalence in the general population and among patients with and without Kaposi's sarcoma. J Virol 74: 3478–3485.

Kazanji M, Dussart P, Duprez R, Tortevoye P, Pouliquen JF, Vandekerkhove J, Couppie P, Morvan J, Talarmin A, Gessain A. 2005. Serological and molecular evidence that human herpesvirus 8 is endemic among Amerindians in French Guiana. J Infect Dis 192: 1525–1529.

Kondo Y, Izumi T, Yanagawa T, Kanda H, Katano H, Sata T. 2000. Spontaneously regressed Kaposi's sarcoma and human herpesvirus 8 infection in a human immunodeficiency virus-negative patient. Pathol Int 50:340–346.

Lacoste V, Kadyrova E, Chistiakova I, Gurtsevitch V, Judde JG, Gessain A. 2000. Molecular characterization of Kaposi's sarcoma-associated herpesvirus/human herpesvirus-8 strains from Russia. J Gen Virol 81:1217–1222.

Meng YX, Spira TJ, Bhat GJ, Birch CJ, Druce JD, Edlin BR, Edwards R, Gunthel C, Newton R, Stamey FR, Wood C, Pellett PE. 1999. Individuals from North America, Australasia, and Africa are infected with four different genotypes of human herpesvirus 8. Virology 261:106–119.

Meng YX, Sata T, Stamey FR, Voevodin A, Katano H, Koizumi H, Deleon M, De Cristofano MA, Galimberti R, Pellett PE. 2001. Molecular characterization of strains of Human herpesvirus 8 from Japan, Argentina and Kuwait. J Gen Virol 82:499–506.

Minoda H, Usui N, Sata T, Katano H, Serizawa H, Okada S. 2006. Human Herpesvirus-8 in Kaposi's Sarcoma of the Conjunctiva in a Patient with AIDS. Jpn J Ophthalmol 50:7–11.

Moore PS, Chang Y. 2001. Kaposi's sarcoma-associated herpesvirus. In: Knipe DM, Howley PM, editors. Fields Virology 4th ed. Philadelphia: Lippincott Williams & Wilkins, pp 2803–2834.

Poole LJ, Zong JC, Ciufo DM, Alcendor DJ, Cannon JS, Ambinder R, Orenstein JM, Reitz MS, Hayward GS. 1999. Comparison of genetic variability at multiple loci across the genomes of the major subtypes of Kaposi's sarcoma-associated herpesvirus reveals evidence for recombination and for two distinct types of open reading frame K15 alleles at the right-hand end. J Virol 73:6646–6660.

Russo JJ, Bohenzky RA, Chien MC, Chen J, Yan M, Maddalena D, Parry JP, Peruzzi D, Edelman IS, Chang Y, Moore PS. 1996. Nucleotide sequence of the Kaposi sarcoma-associated herpesvirus (HHV8). Proc Natl Acad Sci USA 93:14862–14867.

Sato-Matsumura KC, Matsumura T, Nabeshima M, Katano H, Sata T, Koizumi H. 2001. Serological and immunohistochemical detection of human herpesvirus 8 in Kaposi's sarcoma after immunosuppressive therapy for bullous pemphigoid. Br J Dermatol 145:633–637.

Suda T, Katano H, Delsol G, Kakiuchi C, Nakamura T, Shiota M, Sata T, Higashihara M, Mori S. 2001. HHV-8 infection status of AIDS-unrelated and AIDS-associated multicentric Castleman's disease. Pathol Int 51:671–679.

Tachikawa N, Goto M, Gatanaga H, Katano H, Oka S, Wakabayashi T, Mori S, Iwamoto A. 1996. Herpesvirus-like DNA sequences in Japanese patients with AIDS-related Kaposi's sarcoma. J Infect Chemother 1:190–192.

Ueno T, Mitsuishi T, Kimura Y, Kato T, Hasegawa H, Katano H, Sata T, Kurane S, Kawana S. 2007. Immune reconstitution inflammatory syndrome associated with Kaposi's sarcoma: Successful treatment with interferon-alpha. Eur J Dermatol 17:539–540.

Yamada Y, Funasaka Y, Nishioka E, Okuno T, Ichihashi M. 2000. A case of classic Kaposi's sarcoma in a Japanese man: Detection of human herpes virus 8 (HHV-8) infection by means of polymerase chain reaction and immunofluorescence assay. J Dermatol 27:391–396.

Yoshii N, Kanekura T, Eizuru Y, Setoyama M, Kanzaki T, Yamanishi K. 2006. Transcripts of the human herpesvirus 8 genome in skin lesions and peripheral blood mononuclear cells of a patient with classic Kaposi's sarcoma. Clin Exp Dermatol 31:125–127.

Zong JC, Metroka C, Reitz MS, Nicholas J, Hayward GS. 1997. Strain variability among Kaposi sarcoma-associated herpesvirus (human herpesvirus 8) genomes: Evidence that a large cohort of United States AIDS patients may have been infected by a single common isolate. J Virol 71:2505–2511.

Zong JC, Ciufo DM, Alcendor DJ, Wan X, Nicholas J, Browning PJ, Rady PL, Tyring SK, Orenstein JM, Rabkin CS, Su IJ, Powell KF, Croxson M, Foreman KE, Nickoloff BJ, Alkan S, Hayward GS. 1999. High-level variability in the ORF-K1 membrane protein gene at the left end of the Kaposi's sarcoma-associated herpesvirus genome defines four major virus subtypes and multiple variants or clades in different human populations. J Virol 73:4156–4170.

Zong J, Ciufo DM, Viscidi R, Alagiozoglou L, Tyring S, Rady P, Orenstein J, Boto W, Kalumbuja H, Romano N, Melbye M, Kang GH, Boshoff C, Hayward GS. 2002. Genotypic analysis at multiple loci across Kaposi's sarcoma herpesvirus (KSHV) DNA molecules: Clustering patterns, novel variants and chimerism. J Clin Virol 23:119–148.

Ligand-independent higher-order multimerization of CXCR4, a G-protein-coupled chemokine receptor involved in targeted metastasis

Makiko Hamatake, Toru Aoki, Yuko Futahashi, Emiko Urano, Naoki Yamamoto and Jun Komano[1]

AIDS Research Center, National Institute of Infectious Diseases, 1-23-1 Toyama, Shinjuku-ku, Tokyo 162-8640, Japan

(Received July 19, 2008/Revised September 1, 2008/Accepted September 7, 2008/Online publication October 31, 2008)

CXCR4, a G-protein-coupled receptor of CXCL12/stromal cell-derived factor-1α, mediates a wide range of physiological and pathological processes, including the targeted metastasis of cancer cells. CXCR4 has been shown to homo-oligomerize in several experimental systems. However, it remains unclear with which domains CXCR4 interacts homotypically, and whether it dimerizes or forms a higher-order complex. To address these issues, we used bioluminescent resonance energy transfer and bimolecular fluorescence complementation analyses to measure the homotypic interactions of CXCR4 in living cells. Both assays indicated that CXCR4 interacts homotypically, which is consistent with previous studies. By studying CXCR4 mutants lacking various domains, we found that multiple transmembrane domains probably serve as potential molecular interaction surfaces for oligomerization. The relative contribution of the amino- or carboxy-termini to oligomerization was small. To differentiate between a dimer and a multimer consisting of more than two molecules, bioluminescent resonance energy transfer–bimolecular fluorescence complementation analysis was conducted. It revealed that CXCR4 engages in higher-order oligomerization in a ligand-independent fashion. This is the first report providing direct experimental evidence for the higher-order multimerization of CXCR4 *in vivo*. We hypothesize that CXCR4 distributes to the cell surface as a multimer, in order to effectively sense, with increased avidity, the chemotaxis-inducing ligand in the microenvironment. Studying the structure and function of the oligomeric state of CXCR4 may lead us to develop novel CXCR4 inhibitors that disassemble the molecular cluster of CXCR4. (*Cancer Sci* 2009; 100: 95–102)

CXCR4, a widely expressed chemokine receptor of CXCL12/stromal cell-derived factor (SDF)-1α, plays a role in various physiological and pathological processes, including neuronal network development, normal and malignant cell migration, inflammatory reactions, the genetic immunodeficiency syndrome WHIM (warts, hypogammaglobulinemia, infections, myelok-athexis), and human immunodeficiency virus (HIV)-1 infection.[1–7] The CXCR4–CXCL12/SDF-1α axis is reportedly involved in the tumor progression of breast cancer and more recently of pancreatic, esophageal, prostate, thyroid, colorectal, and cutaneous cancers.[8–16] Thus, it has been emphasized that the CXCR4–CXCL12/SDF-1α axis may be an important therapeutic target.[9,14] Understanding the regulatory mechanisms of CXCR4 functions may provide clues to develop therapeutic approaches for such disorders.

CXCR4 was shown to homo-oligomerize by several experimental systems. It is possible that CXCR4 dimerizes because CXCL12/SDF-1α forms a dimer, as indicated by structural analyses.[17–19] However, past biophysical analyses did not critically distinguish between dimers and complexes consisting of more than two molecules (the higher-order oligomer).[20–23] The oligomerization of G protein-coupled recepters (GPCR) has been suggested to play a role in ligand-initiated signaling and protein trafficking, including egress from the endoplasmic reticulum (ER) or internalization from the plasma membrane.[24,25] It appears that steady-state oligomerization and its functional significance vary among GPCR species. Although it is known to homo-oligomerize, the functional significance of CXCR4 oligomerization is not well understood. Isolating a monomeric CXCR4 mutant is one straightforward approach toward understanding the functional significance of CXCR4 oligomerization. However, to achieve this goal, it remains to be clarified whether CXCR4 dimerizes or forms a higher-order complex, and with which domains CXCR4 interacts homotypically. Additionally, it is unknown how selfoligomerization is regulated.

It is hypothesized that, for most mammalian GPCR, the stable homotypic interaction is mediated by a specific transmembrane domain (TMD), as has been shown for some GPCR (e.g. dopamine D2 receptor, adenosine A2A receptor, and CCR5).[26–28] If CXCR4 forms a dimer, it is postulated that two CXCR4 molecules should face each other in a symmetrical configuration on the two-dimensional plane of the biological lipid bilayer (Fig. 1a). If this were the case, it might not be difficult to isolate a CXCR4 mutant lacking TMD that fails to interact homotypically. However, if CXCR4 has multiple interaction facets that multimerize, monomeric CXCR4 mutants may be hard to isolate by the simple mutagenesis approach (Fig. 1b).

To measure TMD–TMD interactions, we used bioluminescent resonance energy transfer (BRET) and bimolecular fluorescence complementation (BiFC) assay systems[29,30] that allowed us to measure the specific homotypic and heterotypic interactions of membrane proteins bearing multiple TMD in living mammalian cells. By analyzing a series of CXCR4 mutants using these two techniques, we found that CXCR4 forms a steady-state molecular cluster consisting of more than two molecules, and that this cluster formation is not mediated by the amino- or carboxy-termini. This is the first report to provide direct experimental evidence that CXCR4 engages in higher-order multimerization *in vivo*.

Materials and Methods

Plasmids. The plasmids pCXCR4, pCXCR4-GFP, and d-31-GFP were described previously.[31] The following oligonucleotides encoding the myristoylation and palmitoylation signal region of *lyn* were annealed and cloned into the *Eco*RI and *Bam*HI sites of pDsRed2-N1 (Clontech, Palo Alto, CA, USA), generating pLynDsRed2: sense, 5′-AATTGCCACCATGGGATGTATTAAA-TCAAAAAGGAAAGAC-3′ and antisense, 5′-GATCGTCTTTC-CTTTTTGATTTAATACATCCCATGGTGGC-3′. The *Sna*BI–*Age*I fragment from pLynDsRed2 was cloned into the corresponding sites of pEGFP-C2, generating pMEM-GFP. The 5′ *Nhe*I end of

[1]To whom correspondence should be addressed. E-mail: ajkomano@nih.go.jp

doi: 10.1111/j.1349-7006.2008.00997.x

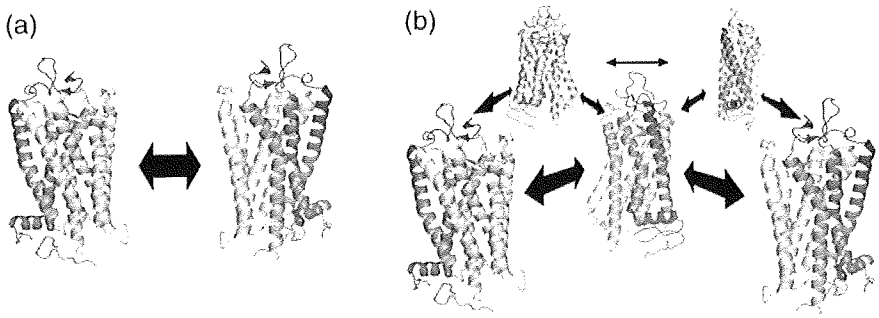

Fig. 1. Hypothetical models of CXCR4 oligomerization. (a) If CXCR4 forms a dimer, it is postulated that two CXCR4 molecules would physically associate with each other via the specific side of the molecule where the same key transmembrane helices are situated. (b) If CXCR4 forms a higher-order multimerization consisting of more than two molecules, CXCR4 should have multiple interaction domains. These models were drawn based on the bovine rhodopsin structure.

the *Nhe*I–*Xba*I fragment from phRL/CMV (Promega, Madison, WI, USA) encoding renilla luciferase (hRL) was ligated to the annealed oligonucleotides of 5′-AGATCTGGTTACCCAATT-3′ and 5′-CTAGAATTGGGTAACCAGATCT-3′. The 3′ end of the same fragment was ligated to the annealed oligonucleotides of 5′-CTAGGATCTGAATTCAGATCT-3′ and 5′-AGATCTGAATTCAGATC-3′. The *Bgl*II fragment was cloned into the *Bgl*II and *Bam*HI sites of pEGFP-C3 (Clontech), generating pEGFP-hRluc. The plasmid pCXCR4 FL-Rluc was constructed by cloning the *Mfe*I fragment from pEGFP-hRLuc BRET into the *Eco*RI and *Mfe*I sites of pCXCR4.

5TMDΔ23 was amplified by a two-step polymerase chain reaction (PCR). In the first step, PCR products were amplified by two separate PCR using the following two primer pairs targeting full-length CXCR4: R4 forward 5′-ACCGGTGCCACCATGGAGGGGGATCAGTATATACACTTCAG-3′ and 5TMDΔ23 reverse 5′-GGGATCCAGACGCCAACATAGACCACCTTGTCCGTCATGCTTCTCAGTTTCTTC-3′; 5TMDΔ23 forward 5′-GAAGAAACTGAGAAGCATGACGGACAAGGTGGTCTATGTTGGCGTCTGGATCCC3′ and R4 reverse 5′-AGATCTCGCTGGAGTGAAAACTTGAAGACTCAGACTC-3′. The second PCR step was carried out by mixing the two first-step PCR products and amplifying the DNA with the R4 forward and R4 reverse primers. The final PCR product was cloned into pCRblunt2-TOPO (Invitrogen, Tokyo, Japan) and sequenced. The *Age*I–*Bgl*II fragment, encoding 5TMDΔ23, was cloned into the *Age*I and *Bgl*II sites of pCXCR4-GFP and pCXCR4 FL-Rluc, generating pCXCR4 5TMDΔ23-GFP and pCXCR4 5TMDΔ23-Rluc, respectively. The 5TMDΔ12, 5TMDΔ34, 5TMDΔ34, and 5TMDΔ34 derivatives were generated similarly by using the following primers: 5TMDΔ12 forward 5′-CCGTGAAGAAAATGCTAATTTCAATAAAGCAGTCCATGTCATCTACACAGTTAACCTC-3′, 5TMDΔ12 reverse 5′-GAGGTTAACTGTGTAGATGACATGGACTGCTTTATTGAAATTAGCATTTTCTTCACGG-3′, 5TMDΔ34 forward 5′-CTGGTACTTTGGGAACTTCCTATGCAAGCACATCATGGTTGGCCTTATCCTGCC-3′, 5TMDΔ34 reverse 5′-GGCAGGATAAGGCCAACCATGATGTGCTTGCATAGGAAGTTCCCAAAGTACCAG-3′, 5TMDΔ45 forward 5′-GGCCAAGGAAGCTGTTGGCTGAAAAGACCACAATCATCCCCATCCTGGCTTTC-3′, 5TMDΔ45 reverse 5′-GAAAGCCAGGATGGGGATGATTGTGGTCTTTTCAGCCAACAGCTTCCTTGGCC-3′, 5TMDΔ67 forward 5′-GTCCTGCTATTGCATTATCATCTCCAAATTTAAAACCTCTGCCCAGCACGCACTC-3′, and 5TMDΔ67 reverse 5′-GAGTGCGTGCTGGGCAGAGGTTTTAAATTTGGAGATGATAATGCAATAGCAGGAC-3′. The 3TMD125 and 3TMΔ367 derivatives were constructed by conducting a two-step PCR using the 5TMDΔ34 forward and reverse primers with 5TMDΔ67 and 5TMDΔ12 as templates, respectively.

The plasmid pCXCR4 d-31-Rluc was constructed by replacing the *Age*I–*Bgl*II region of pCXCR4-Rluc with the *Age*I–*Bgl*II fragment from pCXCR4 d-31-GFP. The plasmid pCXCR2/444 has been described previously,[32] and the *Sna*BI–*Bam*HI fragment from pCXCR2/444 replaced the *Sna*BI–*Bam*HI region of pCXCR4-GFP, generating pCXCR2/4-GFP.

The following oligonucleotides encoding the amino-terminal myristoylation signal region of *lyn* were annealed and cloned into the *Eco*RI and *Bam*HI sites of pEGFP-N1, generating pLyn-GFP: sense 5′-AATTGCCACCATGGGAGCTATTAAATCAAAAAGGAAAGAC-3′ and antisense 5′-GATCGTCTTTCCTTTTTGATTTAATAGCTCCCATGGTGGC-3′. The plasmid pLyn-R4cyt-GFP was constructed by cloning the *Xma*I fragment of a PCR product amplified by 5′-CCCGGGGAAATTTAAAACCTCTGCCC-3′ and 5′-CCCGGGCTGGAGTGAAAACTTGAAG-3′ using pCXCR4-GFP as a template into the *Age*I site of pLynGFP.

CXCR3 was amplified from RNA extracted from human peripheral blood mononuclear cells by reverse transcription-PCR using the following primers; 5′-ACCGGTGCCACCATGGTCCTTGAGGTGAGTGACC-3′ and 5′-GAGCTCGAGATCTCCAAGCCCGAGTAGGAGGCCTCTG-3′. CXCR2 was amplified from a plasmid carrying the CXCR2 open reading frame by PCR using the following primers: 5′-GCCACCGGTGCCACCATGGAAGATTTTAACATGG-3′ and 5′-CCTCGAGCCGAGAGTAGTGGAAGTGTGCCCTG-3′. The *Age*I and *Xho*I fragments encoding CXCR2 and CXCR3 were further cloned into the corresponding sites of pCXCR4-GFP and pCXCR4-Rluc, generating pCXCR2-GFP and pCXCR3-GFP, and pCXCR2-Rluc and pCXCR3-Rluc, respectively. The *Bgl*II and *Mfe*I fragments from phmKGN-MN or phmKGC-MN encoding the fragments of Kusabira-Green (mKG) (MBL, Nagoya, Japan) were cloned into the corresponding sites of pCXCR4-GFP, generating pCXCR4-mKGN and pCXCR4-mKGC, respectively. The *Xho*I and *Mfe*I fragments from phmKGN-MN and phmKGC-MN were cloned into the corresponding sites of pCXCR3-GFP, generating pCXCR3-mKGN and pCXCR3-mKGC, respectively.

Cells, transfection, and imaging. All mammalian cells were maintained in RPMI-1640 (Sigma, St Louis, MO, USA) supplemented with 10% fetal bovine serum (Japan Bioserum, Tokyo, Japan), 50 U/mL penicillin, and 50 μg/mL streptomycin (Invitrogen). Cells were incubated at 37°C in a humidified 5% CO_2 atmosphere. Cells were transfected with Lipofectamine 2000 according to the manufacturer's protocol (Invitrogen). Cells were imaged by confocal microscopy as described previously.[31]

Western blotting. Western blotting was carried out according to techniques described previously,[33] except that the cells were processed with an M-PEK kit according to the manufacturer's protocol (Calbiochem, Darmstadt, Germany). The antibodies used are as follows: a monoclonal anti-FLAG epitope (M2; Sigma), a monoclonal anti-GFP antibody (MAB3580; Chemicon International, Temecula, CA, USA), a monoclonal anti-Rluc antibody (MAB4400 and MAB4100; Chemicon), and EnVision$^+$ (Dako, Glostrup, Denmark).

Bioluminescent resonance energy transfer assay. 293T cells grown in a six-well plate were transfected with 0.05–0.2 μg renilla luciferase (Rluc) derivatives along with 1–2 μg of the green fluorescent protein (GFP) fusion derivative expression plasmids. Varying amounts of plasmids were used to control the expression levels of GFP and Rluc in the transfected cells. At 2 days after transfection, cells were collected and incubated with the Rluc

doi: 10.1111/j.1349-7006.2008.00997.x